April 2020

Hybrid Electro-Plasmonic Stimulation of Primary Neurons

Ratka Damnjanovic
University of South Florida

Hybrid Electro-Plasmonic Stimulation of Primary Neurons

by

Ratka Damnjanovic

A dissertation submitted in partial fulfillment
of the requirements for the degree of
Doctor of Philosophy in Biomedical Engineering
Department of Medical Engineering
College of Engineering
University of South Florida

Co-Major Professor: Robert D. Frisina, Ph.D.
Co-Major Professor: Venkat R. Bhethanabotla, Ph.D.
Joseph P. Walton, Ph.D.
Mark J. Jaroszeski, Ph.D.
Nathan D. Gallant, Ph.D.

Date of Approval:
March 03, 2020

Keywords: Neural Modulation, Trigeminal, Gold Nanoparticles, Visible Light, Prosthetics

Dedication

I want to dedicate this doctoral dissertation to my parents Milica and Ilija Kolev who have always desired and encouraged me to persevere on the course to completion.

This work of extensive labor and great accomplishment I dedicate to them.

Acknowledgments

I would like to express my sincere appreciation and thanks to Profs. Robert Frisina and Venkat Bhethanabotla for their invaluable guidance and help during the course of my project, and my committee members for their support. I am also very thankful to Dr. Parveen Bazard, a Postdoc from Prof. Frisina's lab, for giving me the patch clamp training in the lab and teaching me various experimental procedures, nanoelectrode fabrication and cell line culturing to get me going on my initial patch clamp experiments and for always being there when needed.

Special thanks to Prof. Thomas Taylor-Clark's group at the USF Medical School, especially to Dr. Parmvir Bahia, for teaching me to work with mice neural tissue harvesting and culturing, and for providing the row uncultured mice brain tissue on a regular basis for the duration of the study. This was invaluable source of fresh brain tissue locally on campus.

Many thanks to Drs. Xiaoxia Zhu and Bo Ding and Shannon Salvog for their help in ordering and receiving the chemicals and enzymes for the experiments and lab utilization. Also, many thanks to all my lab mates at USF for being there to help in providing hazard training instructions, IACUC animal and handling certification guidance, and instrumentation help.

I'm very grateful to my company Jabil Healthcare for providing tuition reimbursement support for a portion of my graduate studies and flexibility with my work schedule when needed.

Last but not least, I am very grateful to my family, especially my husband Aleksandar, son Nenad and his wife Daisy, for their encouragement to pursue higher studies at the University of South Florida and for their understanding of my life and career balance during these studies.

Table of Contents

List of Figures

Abstract

Biomedical prosthetics utilizing electrical stimulation have limited, effective spatial resolution due to spread of electrical currents to surrounding tissue, causing nonselective stimulation. So, precise spatial resolution is not possible for traditional neural prosthetic devices, such as cochlear implants. More recently, alternative methods utilize optical stimulation, mainly infrared, sometimes paired with nanotechnology for stimulating action potentials, which has its own drawbacks, as it may heat surrounding tissue. Recently, we employed plasmonic stimulation methods utilizing gold nanoparticle-coated nanoelectrodes to convert visible light pulses into localized surface plasmon resonance transduction for stimulation of electrically excitable cells, which had limited success. Here, we report the development of a next-generation hybrid electro-plasmonic stimulation platform for spatially and temporally precise neural excitation. Trigeminal neurons were co-stimulated *in-vitro* in a whole-cell patch-clamp configuration with sub-threshold-level short duration electrical and visible light pulses (1-5 ms, 1-5 V, 10 Hz) aimed at a gold-nanoparticle coated nanoelectrode placed adjacent to a neuron. Membrane action potentials were recorded with a higher success rate and better post-stimulation cell recovery than with pure optical stimulation, while reducing the electrical stimulus input by up to 40%. Sub-threshold levels of electrical stimuli in conjunction with visible light (532 nm) reliably triggered trains of action potentials. Our hybrid neurostimulation findings open up opportunities for development of new generation high-acuity neural modulation prosthetic devices, tunable for individual needs, which would qualify as preferred alternative over traditional electrical stimulation technologies.

1. Introduction

1.1. Literature Review and Background

Electrical stimulation, although successful at activating neural responses, tends to spread to the surrounding tissues, resulting in non-specific stimulation, making it difficult to stimulate discrete neural sites. To facilitate specific point stimulation, various nanomaterial-assisted neural stimulation approaches have been reported in recent years[1-4] where different localized fields are activated (electric, magnetic, thermal) employing different nanomaterials for stimulation, such as piezoelectric ultrasound waves,[5] magnetic fields,[6] and laser light electromagnetic waves (mainly near-infrared[7-11] and infrared[12]) optical irradiation.

Optical stimulation approaches mainly rely on top-down methodology focused on recording outputs in response to a stimulation input, such as observing muscle contraction as a result of the triggered action potential (AP) response in various animal subjects.[13] More recently, there have been reports of optical stimulation performed in brain tissue slices[14] as well as single cell stimulation of cultured neurons (dorsal root ganglion,[4, 15] spiral ganglion,[16] hippocampal neurons,[17] oocytes[18]). A common approach has been to use infrared (IR) light wavelengths[19] to heat the surrounding aqueous medium sufficiently to induce fast changes in the temperature of the local surroundings, which can heat and stimulate the cell's membrane, presumably triggering membrane capacitive currents.[18]

Although direct heating of the bulk solution has been shown to be effective in triggering action potentials, it is an imprecise way to stimulate neurons as it heats non-specifically and may cause cellular damage. Attempts have been made to modify the stimulation methods and utilize

localized surface plasmon resonance (LSPR) fields for more target-specific heating. Nanoparticle techniques, such as functionalization, bio-conjugation and local injection or deposition of nanoparticles to the target site have been attempted.[4] For example, Parameswaran et al.[15] demonstrated that cathodic photocurrents from single nanowires can elicit action potentials in primary rat dorsal root ganglion (DRG) neurons through a primarily atomic gold-enhanced photoelectrochemical process using coaxial p-type/intrinsic/n-type (PIN) silicone nanowires (SiNWs), where on optical stimulation with 532 nm light illumination at the neuron/PIN-SiNW interface, electrons move towards the n-type shell and holes to the p-type core, inducing a faradaic cathodic process at the n-shell that locally depolarized the target neuron. Carvalho-de-Souza et al.[4] conjugated Au nanoparticles with three different ligands – Ts1 neurotoxin and two antibodies (targeting TRPV1 and $P2X_3$ channel receptors respectively), and successfully bound the particles to dorsal root ganglion neurons, then stimulated the DRGs with 532 nm green laser light. Nakatsuji et al.[20] presented a method using plasma-membrane-targeted gold nanorods (pm-AuNRs) prepared with a cationic protein/lipid complex to activate a thermo-sensitive cation channel, TRPV1, via photothermal heating of TRPV1 on the surface of a single intact neuron using near-infrared (NIR) light. In this study, the highly localized photothermal heat generation, mediated by the pm-AuNRs, induced Ca^{2+} influx solely by TRPV1 activation. Eom et al.[7] conjugated Au nanorods by injection into the rat sciatic nerve using a glass pipette and then excised the nerve bundle and recorded compound nerve action potentials in response to 980 nm IR laser stimulation. Recently, it has been shown that neural cells can be activated more efficiently by pulsed NIR light delivered to gold nanorods (GNRs) near the neural cells, but the mechanisms underlying this GNR-enhanced NIR stimulation have not been explained yet. Eom et al.[21] proposed a model to elucidate the mechanisms by modeling the heat generated from

interactions between NIR light and GNRs, the temperature-dependent ion channels (transient receptor potential vanilloid 1; TRPV1) in the neuronal membrane, and a heat-induced capacitive membrane current. Their results show that NIR pulses induce rapid temperature increases near the neural membrane triggering TRPV1-channel currents and capacitive currents. Both currents collectively increase the generator potential eliciting an action potential, and the stimulus conditions determine which source will be the dominant mechanism, such as the laser pulse duration or the TRPV1 channel density. They concluded that, although the TRPV1 mechanism dominates in most cases, the capacitive current has a greater contribution when a very short laser pulse is used for neural cells with relatively low TRPV1 channel densities. Yoo et al.[10] performed coating of Au nanorods with polyethylene glycol (PEG) to assist binding to the cell membrane, and then invoked inhibition in the rat hippocampal tissue using a 785 nm NIR laser. Li et al.[11] utilized photosensitive hydrogels embedded with polypyrrole (PPy) nanoparticles to release biomolecule transmitters (glutamate & DNQX), and then used 980 nm IR laser light to excite hippocampal neurons *in-vitro* when glutamate was released, and to inhibit responses from the rat visual cortex *in-vivo* when DNQX was released. Yong et al.[8] incubated primary auditory neurons with silica-coated Au nanorods overnight and used 780 nm NIR laser to excite the neurons.

A common theme for these studies is that they employ various modifications of nano-neural interfaces to achieve optical stimulation. The major limitation with these techniques is that they have issues regarding unwanted toxicity, biocompatibility and repeatability. For instance, excessive heating by IR lasers to excite neurons can damage healthy tissues. Therefore, there is a need to find more suitable ways for conversion into new neural prosthetics that would minimize cellular and surrounding tissue damage.

1.2. Motivation: Neural Prosthetics and Cochlear Devices

Research into the use and improvement of neural prosthetic devices to treat and restore sensory function is in high demand. Most neural prosthetic devices, used to restore sensory function, work primarily on the principle of electrical stimulation e.g. cochlear implant for hearing loss[22, 23], retinal implant[24, 25], sacral nerve stimulators for incontinence[26], spinal cord and peripheral nerves stimulators for pain control[27], cardiac pacemakers, etc. Hearing impairment is a highly prevalent neurological and communication disorder in our growing population. According to the World Health Organization's estimates, the number of people with such impairment increased from 42 million in 1985 to about 360 million in 2011 worldwide[28]. And the need for hearing devices is growing. Cochlear implants are associated with an estimated lifetime cost of about US$ 90 000 per child with severe to profound hearing impairment[29, 30]. Even the most advanced hearing devices – cochlear implants, currently available, cannot restore "normal" hearing. Outcomes with the same device vary among patients because of a mix of individual biological, physiological and psychological factors[28].

While the cochlear implant has been a remarkable success in the field of neuroprosthetics, further improvements in the technology are limited by the cochlear implant's dependence on electric current, which tends to spread to the surrounding tissue[31], resulting in non-specific stimulation and low spatial resolution of the stimulus and ultimately limiting the number of physiologically independent stimulation channels that can be achieved[32-34]. Because of currents spread, it has been difficult to stimulate discrete auditory nerve fibers (ANFs) according to respective frequencies. There has been interest in improving the efficacy of electrical stimulation or developing alternative techniques without the disadvantages and limitation of electrical stimulation and the lack of spatial specificity[35]. Similarly, neuroscience

would benefit from the ability to turn individual neurons on or off[36]. Therefore, continued development of novel modes of stimulation that can allow more precise spatial control of excitation sites is very important and in demand.

The recent studies have proposed to replace electrical electrodes in a cochlear implant with optical radiation sources, and more specifically with infrared radiation[37], with the intent of stimulating more discrete populations of neurons. Infrared neuron stimulation (INS) has been tried to stimulate auditory nerve fibers (ANFs) of deaf animals, giving better spatial resolution as compared to electric stimulation[38-41]. It was concluded that the likely mechanism by which optical INS stimulation occurs is a small, transient increase in tissue temperature upon light absorption by water[42, 43], causing local temperature rise which changes the membrane capacitance, leading to depolarization of the neurons[44]. Despite mounting evidence from animal studies that INS can be used to modulate biological function, it has also been shown that it can have detrimental effects due to overheating of surrounding tissue, which can cause thermal damage or unwanted stimulation[42]. Recent *in vivo* data, however, suggest that cells co-stimulated electrically and optically show a greater response than with optical INS alone[45].

2. Objectives

2.1. Research Objectives

The goal of this research was to show that the plasmonic properties of metal (Au) nanoparticles and visible wavelength light can be used to stimulate primary neurons to improve stimulus spatial resolution. For that matter, an Au nanoelectrode (AuNPs-coated quartz micropipette) was used, which did not need any bio-conjugation or surface modifications of the nano-neural interface to achieve neural excitation. This nanoelectrode was previously characterized and validated for generation of plasmonic responses by Bazard et al.[46] by stimulating two different types of known electrically excitable cells, SH-SY5Y human neuroblastoma cell line that has characteristics of neurons, and neonatal cardiomyocytes. The present work investigated stimulating primary neurons, more specifically primary mouse trigeminal neurons. Like our previous report[46], there was success with pure optical stimulation, but a minority of neuron cells responded to the optical stimuli alone, and detrimental effects were generally observed on cells with higher levels of pure optical stimulation.

In addition, this study goes one step further where optical plasmonic stimulation is paired with electrical, for a novel type of hybrid stimulation, with tunable properties. In the present work, specifically we investigate plasmonic localized heating stimulation as a baseline for the later hybrid stimulation of trigeminal primary neurons from postnatal mice using gold nanoparticles and visible laser light. The ultimate goal being to evaluate if visible green light (532 nm, 1-5 ms pulses) could be used in conjunction with reduced levels of electrical stimulation to stimulate primary neurons, hypothesizing that the detrimental effects could be

reduced by the proposed combination. This approach was successful, and the results demonstrated that optical stimulation can be used in conjunction with sub-threshold electrical stimuli, to consistently activate primary neurons with improved success rates, repeatability & reproducibility. Preliminary results show that applied pulses of the combination hybrid stimulation (laser + electric current pulses) significantly lowered the input current requirement compared to the pure electrical modality stimulation. AP responses obtained were higher in amplitude with shorter time duration compared to optical plasmonic stimulation alone.

The current study therefore expands on the earlier study done with SH-SY5Y human neuroblastoma-like cancer cells by achieving *in-vitro* plasmonic stimulation as well as hybrid stimulation action potential response from primary trigeminal neurons from postnatal mice and optimizing the cellular response modes.

2.1.1. Hypothesis

Tunable pulse delivery of a combined plasmonic and electrical stimulus will evoke membrane action potential response with higher success rate and better post-stimulation cell recovery as compared to pure optical stimulation.

2.1.2. Specific Aims

a) Obtain action potential recording while reducing the electrical stimulus by 30-40% as plasmonic stimulus is added for a hybrid stimulation.
b) Optimize the plasmonic to electrical stimulus ratio to achieve highest success rate of post-hybrid electrical action potential recording with least damage to the cells i.e. higher survival rate.

2.1.3. Proof of Concept

The intention of this research is that these findings can serve as initial *in-vitro* proof of concept for optical plasmonic stimulation of primary neurons, and more specifically trigeminal neurons, using the LSPR phenomena, as well as *in-vitro* proof of concept for hybrid electro-plasmonic stimulation for stimulation of primary neurons. The plasmonic stimulation was achieved by illuminating the AuNPs-coated nanoelectrode, positioned adjacent to the neuron (~2 μm), with a 532 nm green laser light. The hybrid electro-plasmonic stimulation was employed to elicit similar action potential (AP) responses in primary trigeminal neurons with less energy at the subthreshold level. The plan was to show how various combinations of pulse durations, through repetitive bursts of electrical and plasmonic pulses at the subthreshold level, modulate neural firing patterns in primary neurons to achieve cellular AP responses with improved firing success rates, survival rates and repeatability, while significantly reducing the negative side effects, such as the overheating of surrounding tissue as with IR laser light, or the poor specificity as with electrical stimulation alone.

2.1.4. Trigeminal Neurons Selection

The present study expands our previous plasmonic stimulation findings into a wider proof of concept arena; this time using primary trigeminal neurons cultured from 5-7 week-old C57Bl/6 mice to demonstrate applicability and reproducibility. Specifically, the trigeminal neurons were chosen for culturing and stimulation for this research due to their wide array of functions. The trigeminal nerve is the fifth cranial nerve and the principle sensory nerve of the head that innervates the nasal cavity, paranasal sinuses, oral mucosa and the skin of the face, as well as the cerebral arteries and the dura mater. As such, the trigeminal neuron has mixed

sensory, motoric and parasympathetic functions, with a large sensory root and a smaller motor root, which sprout from the side of the pons into three branches as follows: 1) Ophthalmic (CN V1) and 2) Maxillary (CN V2) general sensory components and 3) Mandibular (CN V3) general sensory and branchial motor components[47]. The trigeminal nerve is in constant communication with the autonomic nervous system, including the ciliary, sphenopalatine, otic, and submaxillary ganglia and the oculomotor, facial, and glossopharyngeal nerves[48]. In addition, the trigeminal nerve conveys information to key areas in the brain, including the locus coeruleus, the nucleus solitarius, the vagus nerve and the cerebral cortex. The trigeminal nerve also sends signals to the anterior cingulate cortex, which is involved in attention, mood and decision-making.

2.2. Preliminary Work and Baseline

First, the previously conducted experiments by our group with SH-SY5Y neuroblastoma cell-line have been partially reproduced at the start of the current project, per the patch clamp procedure and culturing protocol described below, with the aim to show reproducibility and to gain the necessary skillset required to perform the patch clamping, in preparation for the later experiments with primary neurons as part of the ultimate goal of the current project.

The SH-SY5Y human neuroblastoma cell-line, which has characteristics of neurons, was therefore plasmonically stimulated using a 532 nm visible light delivered via a monofilament laser fiber aimed at the tip of the gold nanoparticle-coated micropipette (nanoelectrode) positioned next to a patched cell, and neural responses were recorded. It was reconfirmed that wireless nanoelectrode in combination with visible light can be used to stimulate neural cellular responses.

2.2.1. Cell Culture and Differentiation of SH-SY5Y Neuroblastoma Cells

SH-SY5Y (ATCC®CRL-2266) neuroblastoma cell lines were differentiated to neurons in presence of retinoic acid. The cells were initially cultured in a special medium which is mixture of F12 & DMEM (1:1, volume/volume - v/v) containing 10% FBS and 1% PenStrep at 37ºC with 5 % CO2. The medium was changed every 4-7 days. After 80-90% confluence, the trypsin was added to detach the cells. The cells in trypsin solution were incubated for 1-2 minute. Then, an equal volume of medium, DMEM: F12 (1:1 v/v) with 10% FBS & 1% PenStrep, was added to neutralize the trypsin. The cells were centrifuged at 1500 rpm for 5 min. Next, the cell pellet was suspended in 90% FBS, 10% DMSO for long-term storage in 1.5 ml screw cap vials in a liquid nitrogen cylinder. For the subculture, cell pellets were suspended in medium, DMEM: F12 (1:1, v/v), 10% FBS, 1% PenStrep. After 48 h of plating, the DMEM medium was replaced with the Neurobasal medium containing supplements B27 and GlutaMAX. 10 mM all-trans-retinoic acid (ATRA) was added to this medium to promote differentiation. Along with promoting differentiation, the retinoic acid inhibits cell growth as well. The medium was changed every 48 hours[49-51].

The benefits of repeating some of the prior work were to learn cell culturing method for SH-SY5Y cell line, learn the skills to perform patch clamp experiments, learn micropipette pulling and coating procedure, learn the patch clamp equipment setup, and cell action potential recording. The figures below show one such AP recording with the SH-SY5Y cell line.

Figure 1 below shows a patched SH-SY5Y neuroblastoma cell and the AP recordings obtained through electrical and plasmonic stimulation of the stimulated cell.

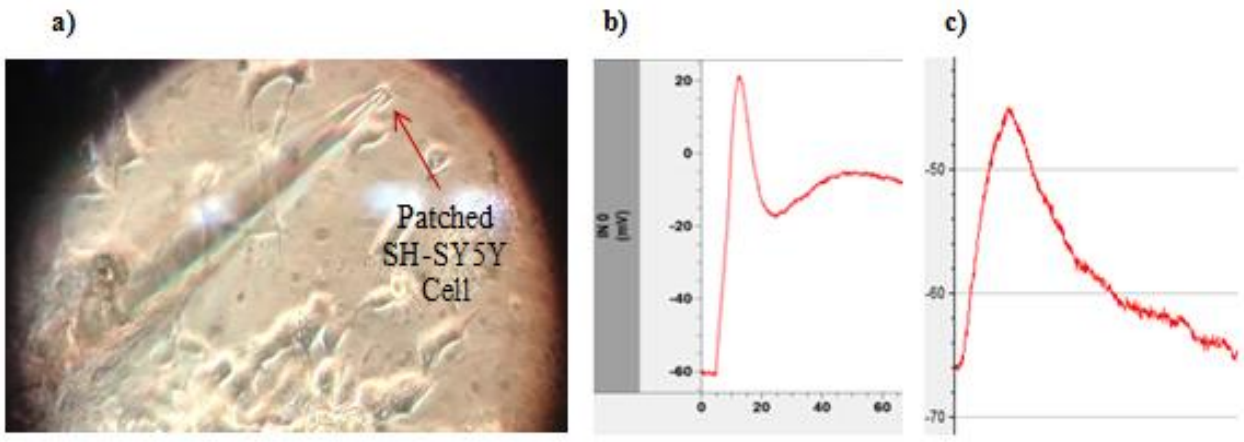

Figure 1. SH-SY5Y Neuroblastoma Cell in Whole Cell Current Clamp Recording Configuration. (a) Digital micrograph of a micropipette over a patched SH-SY5Y cell under 40 X magnification. (b) Action Potential via electrical stimuli. (c) Membrane potential shift during plasmonic laser stimulation (10 ms, 10 Hz, 120 mW).

3. Experimental Methods

3.1. Plasmonic and Hybrid Stimulation Methods

Here we present a new platform for neural stimulation – plasmonic stimulation (PS) combined with electrical stimulation at the sub-threshold level. Gold nanoparticles have been used to coat the plasmonic stimulation nanoelectrodes, since metal nanoparticles, such as the gold, demonstrate Surface Plasmon Resonance (SPR) effect. Biomedical implants based on SPR phenomena have the potential to give better spatial resolution and thus more clinically useful focal stimulation. Compared to the current predominate photothermal neuromodulation modality, direct infrared (IR) laser stimulation, which is susceptible to collateral heating, there is a fundamental difference in transduction, in that the photoabsorber is nanoparticles, as opposed to water, allowing heat distribution to be controlled at the nanoscale. Additionally, photothermal stimulation has the advantage of not generating electrical artifacts that might interfere with concurrent electrical recordings, which are utilized in electrical closed-loop neuroprosthetic systems, as well as in experimental neuroscience. Other groups have recognized the potential for optical plasmonic stimulation of neurons, including Bezanilla & Pepperberg[4], who bound gold nanoparticles (AuNPs) to the cell membrane prior to introducing the optical stimulus. Our group's approach is similar, but utilizes device substrate-bound AuNPs to overcome nanoparticle clearance from the target site and provide a feasible path towards a chronic implant, with the potential to revolutionize active implantable biomedical devices.

The *in-vitro* optical stimulation of the current research will provide basis for such new generation improved implantable devices. The main goal of this project is to investigate this highly localized phenomenon through stimulation of trigeminal neurons to obtain action potentials. Our group will later use this principle to develop a cochlear implant with improved spatial resolution enabled by more selective stimulation of neurons along the frequency axis.

3.2. Synthesis of Gold Nanoparticles

Colloidal gold nanoparticles (spheres) have been synthesized by a citrate method that involves reduction of a gold salt solution (Chloroauric acid HAuCl4·3H2O) by sodium citrate (Na3C6H5O7·2H2O) aqueous solution[52]. Labware cleanliness plays a big role in the successful gold coating synthesis procedure, to eliminate any impurities. Therefore, the glass beakers and magnetic stirrer were washed thoroughly first with distilled water, then, with 190 proof ethanol, and air dried or placed in an oven at 100ºC to dry before use. In a round bottom flask, a 20 ml of 0.1 mM chloroauric acid (HAuCl4) aqueous solution was brought to a vigorous boil on a heating plate with continuous stirring, using a magnetic stirrer. Then, 3 ml of the prepared 1% sodium citrate solution was added rapidly to the boiling solution of chloroauric acid (slow addition would lead to larger particles, which is not desirable in this case). After 10-15 min, with continued stirring, a considerable change in the color of colloidal solution could be observed visually, where the color of the solution changes from pale yellow to colorless, gray, light blue, purple, ruby and finally deep red as shown in Figure 2a), which indicates the presence of Au nanoparticles. After 0.3, 1 and 5 min of reaction time, a change in color begins, which has also been observed analytically in previous work by recording the UV-vis absorption spectra, particularly in the range of 500 - 550 nm[53]. The heat was switched off while continuing the

stirring and allowing the solution to gradually cool down to ambient temperature. No further change in the color of the gold suspension was observed after 60 min of reduction indicating completion of reaction. The colloidal suspension was used immediately after reaching room temperature. It should be filtered through a 022µm PVDF syringe filter (Fisher Scientific).

a)

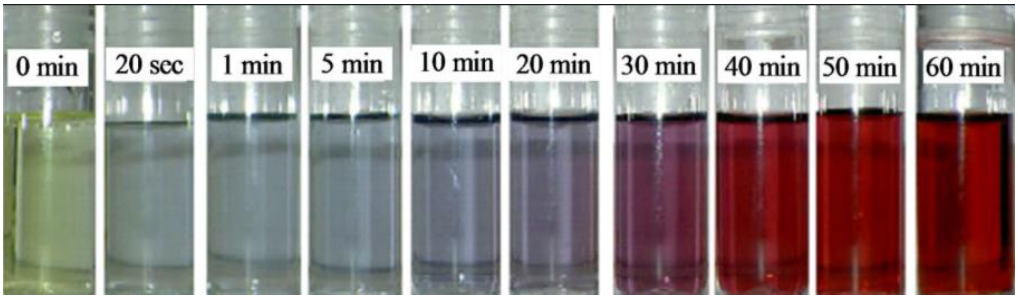

b)

Figure 2. Colloidal Gold Nanoparticle solution. (a) Color changes of solution during course of colloidal AuNPs synthesis with SC as reductant[54]. (b) Color of colloidal gold solution at end of reaction as obtained for this study in our lab.

3.3. Gold Nanoelectrode Fabrication for Neuron Stimulation

Our first-generation Au NPs coated nanoelectrode system consisted of approximately 20 nm diameter colloidal AuNPs coated onto the surface of a glass micropipette, as reported in our previous work.[46] Briefly, colloidal AuNPs (spheres) were synthesized by a citrate method[46, 53, 55-57] that involves reduction of a gold salt solution (Chloroauric acid $HAuCl_4 \bullet 3H_2O$) by sodium citrate ($Na_3C_6H_5O_7 \bullet 2H_2O$) aqueous solution. Spherical AuNPs with 20 nm diameter were chosen because they are easily made with limited size dispersion into a colloidal solution and are generally considered to be biocompatible[58]. The method followed was the one described by Nath & Chilkoti[59] who studied the interaction of a biomolecule with a monolayer of AuNPs coated glass cover-slips. The micropipette coating procedure involved three steps: 1) cleaning the glass surface, 2) functionalization of the glass surface with γ-(aminopropyl) triethoxysilane, and 3) coating of the functionalized glass surface with colloidal AuNPs. We used this method in a similar manner for the current study to coat the synthesized AuNPs onto the borosilicate nanoelectrodes, with prior silanization of the glass pipettes surface using 10% volume solution of γ-(aminopropyl) triethoxysilane) (APTES) in ethanol. The silanized glass electrodes were dipped overnight at room temperature in the synthesized colloidal AuNPs suspension, resulting in a self-arranged chemical deposition of AuNPs coating onto the tip surface of the microelectrodes, which possess plasmonic properties.

3.3.1. Pulling of Micropipettes

The micropipettes used for the patch-clamp recordings were pulled using a glass micropipette puller (P-97, from Sutter Instruments, Novato, CA) by adjusting the pulling parameters to obtain 4-7 MΩ pipette resistance.[60]

A 5 MΩ is the standard resistance used for most recordings. Rationale behind micropipette pulling parameters optimization to obtain certain resistance (Pipette cookbook, Sutter Instruments): Lower resistance pipettes (of 3-4 MΩ) will give a lower series resistance and thus, will be better for voltage-clamp recordings. However, the tip of the glass pipette will be larger than for higher resistance pipettes and, as a consequence, the seal formation will be challenging and the seal will be more difficult to keep stable over time. Higher resistance glass pipettes (of 6-7 MΩ, with a thinner tip) are easier to form a seal with and can be more suitable for prolonged current-clamp recordings; however, they are slightly more difficult to break through the membrane into whole-cell mode and will give a higher series resistance, sometimes too high for reliable voltage-clamp recordings.

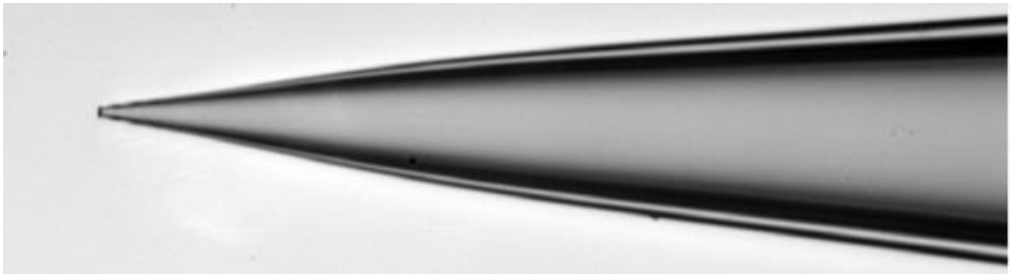

Figure 3. Patch Pipette Profile, 1.5mm x 0.86mm thick walled glass, ~2µm Tip, 3-4mm taper. [61] The ideal morphology for a patch pipette intended for dissociated/cultured cells is a short stubby taper, a high cone angle, and a 2-3 micron tip. This is best generated by using Thick Walled Glass and a 2.5mm or 3.0mm box filament, five loops - Prog #51 (General Look Up Tables) recommended by Sutter Instruments (Pipette cookbook). We used program # 46 to obtain the desired resistance of the pipette.

3.3.2. Cleaning of Micropipettes

The tipped glass micropipettes were plugged at the back with Parafilm wax tape, to prevent capillary suction of the washing liquid and coating into the inside lumen of the pipettes. The pipettes were then taped on the bottom of a plastic petri-dish and the tips soaked into liquid detergent, and then placed on top of a heating plate with continuous heating at 55 − 60ºC for 10-15 min, as shown in Figure 4. Cleaning of micropipettes. Occasional mild shaking was applied to wash off the tips. Next the micropipettes were thoroughly washed with running distilled (DI) water to remove any detergent residue. Then, the micropipettes were cleaned with 1:1 v/v (volume/volume) solution of HCl and methanol for 30 min, by soaking the tips, and subsequently washed with DI water thoroughly. Micropipettes were dried overnight at 60ºC (140 F) in an oven.

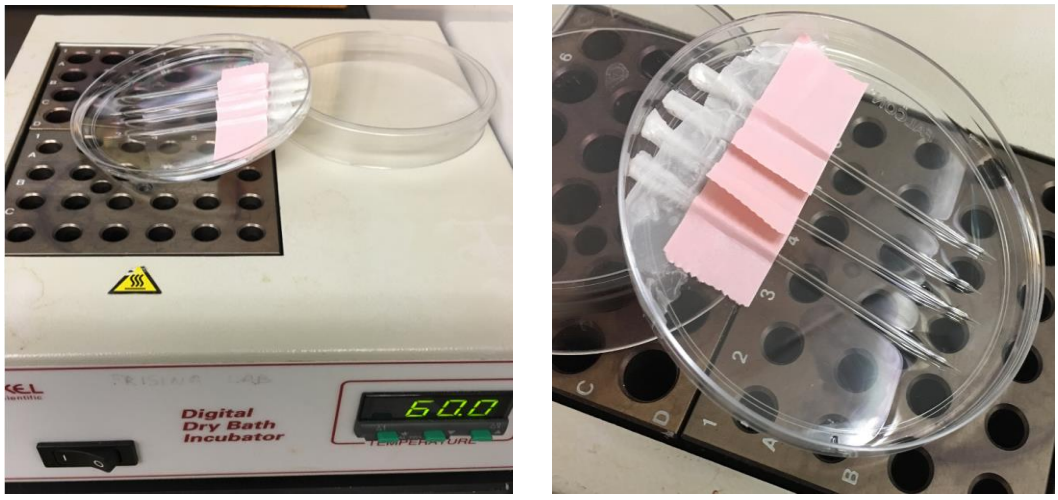

Figure 4. Cleaning of micropipettes by soaking in liquid detergent for 15 min, then rinsing with running distilled (DI) water, followed by soaking again in a 1:1 v/v (volume/volume) solution of HCl and methanol for 30 min, by soaking the tips, and subsequently washed with DI water thoroughly.

3.3.3. Functionalization of the Micropipettes with γ-(Aminopropyl) Triethoxysilane

Glass surface is functionalized (silanized) to prevent adsorption of solute to the glass surface and to increase the hydrophobicity of the surface, which is important to have when dealing with cells. After the washing steps above, the micropipettes were taken out of the oven and the tips of the micropipettes immersed in 10% v/v solution of γ-(aminopropyl) triethoxysilane in anhydrous ethanol (200 proof) for 15 min. Subsequently, the micropipettes were washed five times with ethanol with rigorous shaking motion to mimic sonification, until all residue is removed. After thorough cleaning, the pipettes are transferred into a clean glass petri dish, placed in an oven and dried at 120 ◦C (248 F) for 3 h.

3.3.4. Coating of Gold Nanoparticles

After the functionalization steps above, the micropipettes were taken out of the oven and the tips of the micropipettes immersed for 24 to 36 hours continuous soak in the previously prepared gold nanoparticles solution at room temperature, without any disturbance, lightly covered with a lid to minimize the evaporation and dry out possibility.

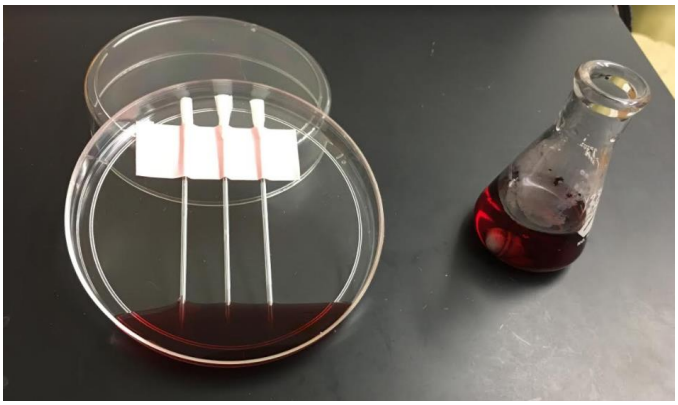

Figure 5. Au NPs coating on glass micropipettes by soaking the tips of the glass pipettes in the colloidal gold nanoparticles solution.

3.4. Patch Clamp Equipment Setup

The Axon Instruments patch-clamp products were used with the complete workflow setup for electrophysiology data acquisition and analysis, as de.

Figure 6. Patch Clamp Equipment Setup digital images. The patch clamp equipment setup consists of a Faraday cage and air/anti-vibration table set to isolate vibration and electrical noise sources, a head-stage device that holds the micropipettes with built-in circuitry to transmit electrical signals from the micropipettes onto the amplifier, a microscope with up to 60x magnification, MPC 200 ROE input and three MPC 265 manipulators, Axopatch 700B amplifier for whole-cell recordings and a Digidata 1440 low-noise data acquisition system.

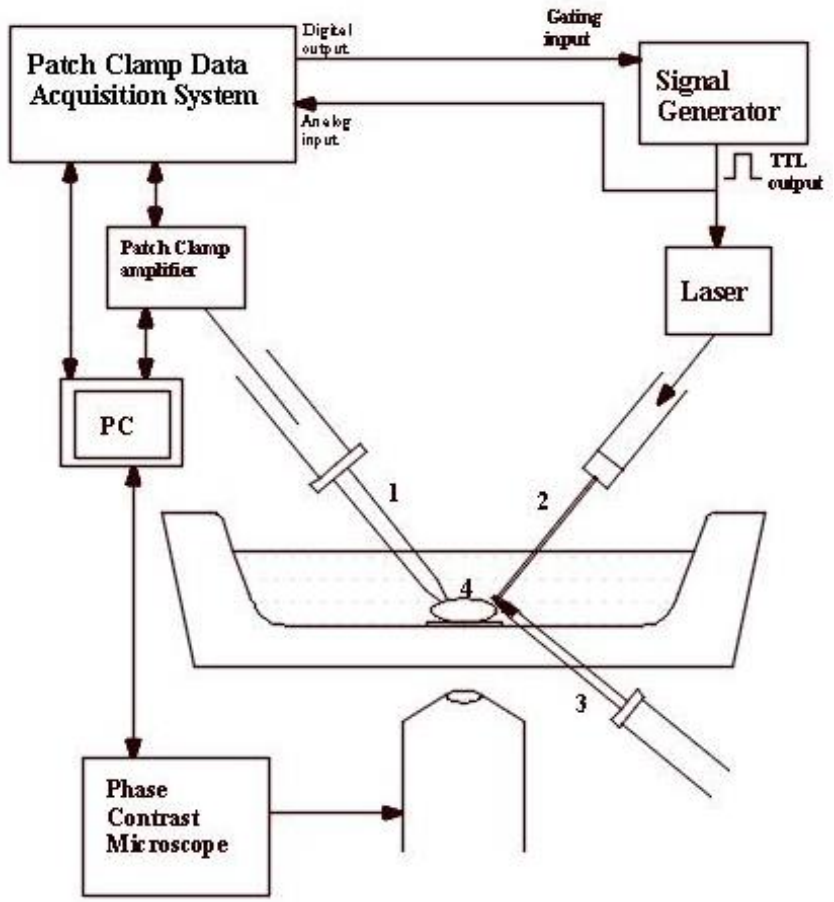

Figure 7. Schematic of the experimental patch clamp equipment setup and electrodes positioning for plasmonic and hybrid stimulation experiments in relation to the patched neuron cell in the petri dish. Whole cell patch-clamp technique used in conjunction with an Axopatch 700B Multiclamp amplifier connected to a patch pipette filled with an intracellular solution (ICS), known as the measuring electrode (1), paired with Digidata 1440A data acquisition interface (Molecular Devices) and pCLAMP-9 software (Axon Instruments, Union City, CA, USA). Extracellular solution (ECS) was used to flood the cells (4) in the petri dish. A 50 µm inside diameter optical fiber (2) was used to focus a 532 nm green laser light onto the surface of the AuNPs coated microelectrode tip (3). The AuNPs coated microelectrode was placed near the cell's surface (~2 µm). For the hybrid stimulation, an electrical stimulus was added via the patch-clamp electrode (1), in addition to the optical plasmonic stimulation generated by the laser beam (2) from the optical fiber (ThorLabs) shining onto the tip of the AuNPs coated microelectrode (3). Neural responses were recorded using the patch-clamp electrode (1).

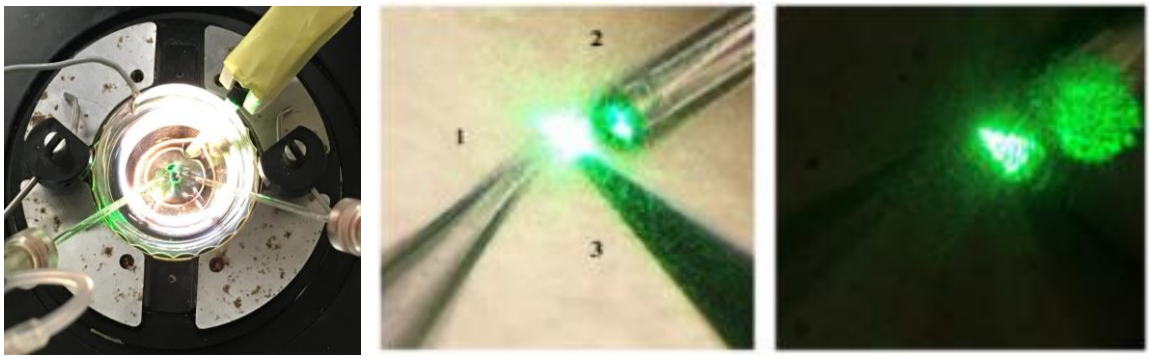

Figure 8. Digital photographs taken of the experimental patch clamp setup when illuminated by the laser beam, as seen inside the petri dish with a naked eye (left), under 5x (middle) and 20x (right) magnifications. The focus is on the position of the electrodes in the petri dish in relation to the patched neuron. The neuron is patched with the measuring electrode (1), while the laser beam is shined upon the tip of the nanoelectrode producing the plasmonic effect. A 50 μm inside diameter optical fiber (2) was used to focus the 532 nm green laser light on the surface of the tip of the AuNPs coated nanoelectrode (3).

3.5. Cell Culture

3.5.1. Coating Coverslips

Coverslips were cleaned in 100% ethanol and then coated with a 5μg/ml coating solution that was made of 50 μl aliquot of laminin (Invitrogen) mixed in 10 ml of poly-d-lysine PDL (0.1 mg/ml) stock solution. The PDL-laminin mix is sterile filtered and applied in quantities of approximately 120 μI PDL/laminin (one small drop) to the center of each coverslip, and left at room temp for at least 30 min. Then the coating is aspirated with a pipette, and the coverslips washed with 200 μI of sterile deionized (DI) water and allowed to dry before use.

3.5.2. Trigeminal Neurons Cell Culturing Protocol

Trigeminal neurons were obtained from the brain of 5-7 week-old C57B1/6 mice. The trigeminal neurons were removed after decapitation and maintained in a cold (4–5°C) Ca^{2+}- and Mg^{2+}-free Hanks' balanced salt solution (HBSS; Gibco BRL, Rockville, MD, USA).

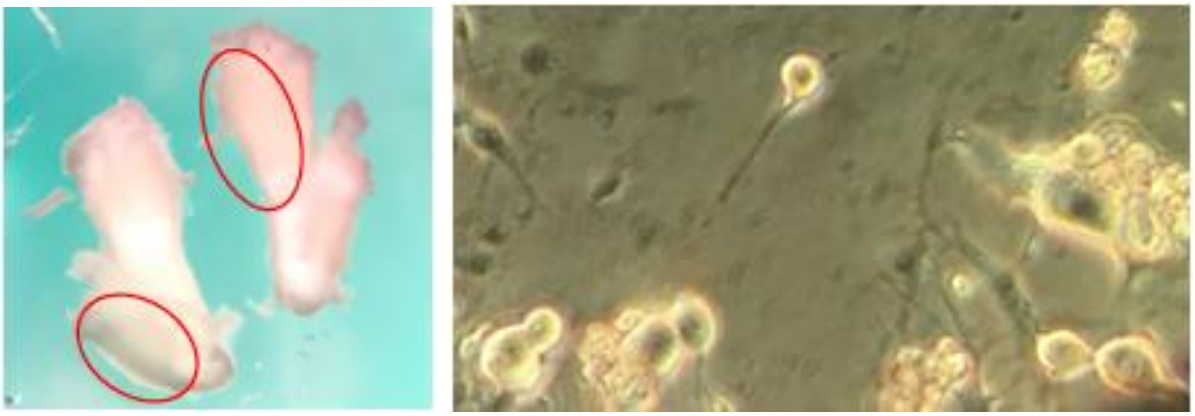

Figure 9. Trigeminal neurons: a) neuron tissue after extraction from the brain's cranial cavity of 5-7 week-old C57B1/6 mice pointing out the location of the trigeminal cell bodies. b) neuron cell culture *in-vitro*

Trigeminal neurons were dissociated enzymatically with HBSS containing collagenase type IA (1mg ml−1, Sigma, St Louis, MO, USA) and dispase II (1 mg ml−1, Boehringer Mannheim, Mannheim, Germany). Enzymes, collagenase type 1 and dispase II (2mg/ml), were dissolved in HBSS and sterile filtered using a white PVDF syringe filter before use. The required solutions were prepared, 40 ml of HBSS, 21 ml of L15+ 10% FBS, and 11 ml L15+FBS. The tubes of L15 were placed in the incubator at 37 ^{o}C, 5 % CO_2 to warm up. Meanwhile, a 20-40 g mouse is euthanized using CO_2 overdose, decapitated and the trigeminal nerves dissected out. The trigeminal ganglia were minced into pieces and left to incubate at 37 °C in the collagenase/dispase II solution for 50 min. During this incubation, coated coverslips were

transferred to a 6-well plate. Coverslips were cleaned in 100% ethanol and then coated with a 5µg/ml laminin mixed in poly-d-lysine (PDL) coating solution. Coverslips were left at room temp for at least 30 min. Then, the coating solution was aspirated with a pipette, and the coverslips washed with 200 µI of sterile deionized (DI) water and allowed to dry before use. The Bunsen burner was set and three glass pipettes were fire polished for trituration - large, medium (10-15 sec to take up solution), and small (45-60 sec to take up solution) size bores. After 30 min of incubation, the neurons are triturated with the wide bore pipette, and then put back into the 37 °C water bath for another 20 min. Finally, they were dissociated with the medium followed by the small-bore pipette. The cell suspension was then, centrifuged at 2200 rpm for 2 min. A 55 µl of pen/strep solution (1:200) is added to the 11 ml of L15+FBS previously left in 37 °C incubator. Next, the HBSS was aspirated and pellet was re-suspended in 10 ml L-15 medium containing 10% FBS and centrifuged again (2200 rpm, 2 min). Medium was aspirated again and cells were re-suspended in 10 ml L-15 medium containing 10% FBS and pen/strep and then centrifuged again (700 g, 2 min). Finally, the medium was aspirated and cells were re-suspended in 100 µl L15+FBS+pen/strep (20 µl per coverslip). Suspension was pipette mixed 50 times with a p200 pipette and transferred in portions of 20 µl suspension to coverslips coated with PDL and laminin. The 6-well plate (culture dishes) was placed in incubator for 1-2 hr to incubate. Then, the wells were toped (flooded) with 2 ml of L15 containing 10% FBS and left to incubate at 37°C. All cells were used within 36 h.

Figure 10 below shows the membrane action potential response of a representative trigeminal neuron when it was patch-clamped in the current clamp configuration, and then stimulated electrically using an electrical current pulse at the threshold level over a prolonged time of exposure (500 ms).

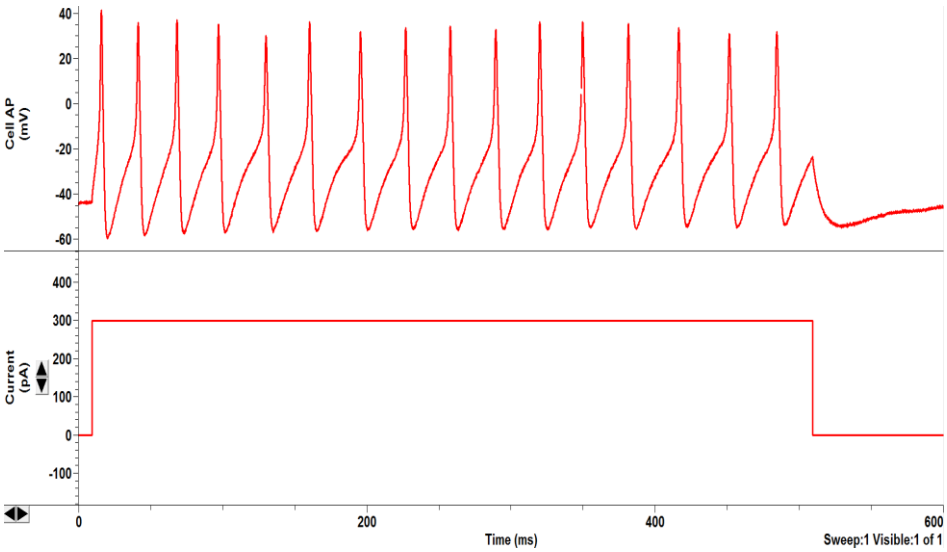

Figure 10. Typical trigeminal neuron action potential response from a representative cell. Electrical stimulation multiple action potentials were recorded when the neuron cell was stimulated with electric current pulse at the threshold level of 300 pA over extended sweep duration of 500 ms. Note: The starting threshold level is relative as it can vary from cell to cell.

3.6. Physiological Solutions

3.6.1. Extracellular Solution (ECS)

Extracellular solution, used to flood the cells in the dish, was prepared with the following composition (mM): 154 NaCl; 4.7 KCl; 1.2 $MgCl_2$; 2.5 $CaCl_2$; 10 N-[2-hydroxyethyl]piperazine-N′-[2-ethanesulphonic acid] (HEPES); pH adjusted between 7.3 and 7.5 with NaOH.

3.6.2. Intracellular Solution (ICS)

Intracellular Solution, used to fill the patch pipettes (4-7 MΩ) using micro syringe, was prepared with the following composition (mM): 140 KCl, 1 $CaCl_2$, 2 $MgCl_2$, 10 N-[2-hydroxyethyl]piperazine-N′-[2-ethanesulphonic acid] (HEPES), 10 (D(+)-Glucose, reagent ACS, Anhydrous), 11 ethylene glycol-bis(β-aminoethyl ether)-N,N,N′,N′-tetraacetic acid (EGTA); pH 7.3 adjusted with KOH.

3.7. Whole Cell Patch Clamp Technique

All electrophysiology experiments and action potential measurements were done using the whole cell patch-clamp technique in conjunction with a Multiclamp 700B amplifier and Digidata 1440 data acquisition interface system (Molecular Devices, Sunnyvale, CA) and a pCLAMP-9 software (Axon Instruments, Union City, CA, USA).

3.7.1. Preparation for patch clamping a neuron

First, a cell is located to patch. The microscope stage should not be disturbed for the rest of the procedure. The borosilicate pipette is filled halfway with an intracellular solution, using a micro syringe and the pipette tapped few times to eliminate any air bubbles that might be present in the tip of the pipette.

3.7.2. Giga-seal formation

The patch-clamp borosilicate glass pipette, having resistance 4-7 MΩ, was filled with intra-cellular solution using a micro syringe and placed in the pipette holder. Before lowering the

pipette, there must be slight pressure on the pipette fluid to blow any contamination in the bathing solutions away from the pipette tip. The pipette tip was placed in the bath filled with extracellular solution and the tip focused under 40 x magnification. A small voltage pulse was applied; 10 mV, 50 ms, 20 Hz, and current responses were recorded. The pipette was then slowly lowered down. When very near to the cell, the movement was stopped, the pipette potential was zeroed, and a little suction applied as needed to patch the cell and form Giga-seal (resistance > 1 G-Ohm).

3.7.3. Whole Cell formation

After a Giga-seal was formed at the neuron cell body, the pipette potential was switched to near the membrane potential, therefore getting access to the cell membrane resistance. A membrane break-through was attempted to achieve the whole cell configuration and get a recording of the cell membrane capacitance. Successful break-through was indicated by the capacitive transient due to membrane capacitance. There was a slight increase in the steady state current. The strategy with medium size pipettes (2-6 M-Ohm) was used in these experiments to get access to the inside of the cell by applying positive pressure to the membrane, in which case a mild suction pulse was applied, without excess force, , using a syringe connected to the patch pipette assembly via a micro-lumen tubing to pull the vacuuming. If whole cell seal was not formed, the zap option was applied immediately through the patch-clamp electronic protocol followed by another suction pulse in an attempt to patch-clamp the membrane. The zap pulse size was increased if needed and a continuous suction applied with an increase in force until the whole-cell seal was formed. Incrementing zap impulses and applying strong suction was used to

secure a good patch. Membrane potentials were measured by switching to current clamp with zero current, canceling the capacitive response.

Seal Resistance was desired to be greater than 1 G-Ohm (GΩ), and series resistance lower than 20 M-Ohm (MΩ) during the recordings. Membrane potential was sought to be more negative than -50 mV for normal potassium intracellular solutions. Ionic composition of intracellular medium was subject to changing as soon as the patch was disrupted, so subsequent measurements were not made. Results are from cells where cell capacitance and resistance were stable, without leaky membranes.

3.7.4. Whole-cell patch-clamp recordings

Patch pipette voltage offset was neutralized prior to the formation of a GΩ seal. Membrane input resistance (Rin), series resistance (Rs), and capacitance (Cm) were determined from current transients elicited by 5 mV hyperpolarizing voltage steps from a holding potential of −60 mV using the membrane test application of pCLAMP-9. In current-clamp mode, holding membrane potential was maintained at −60 to −70 mV. The identification of the AP hump was from the peak value from the recorded AP data. Threshold (TH, the most hyperpolarized potential at which the cell was able to fire an AP) was determined by injecting increments of depolarizing current (Δ of 50-100 pA) for 5 ms pulse width, until the cell starts to elicit AP.

3.8. Plasmonic and Hybrid Electro-optical Stimulation Method

To investigate whether the activity of a single primary neuron can be evoked by plasmonic and hybrid stimulation, an *in-vitro* patch-clamp electrical and optical stimulation and recording platform was utilized. For plasmonic and hybrid stimulations, the Au nanoparticles

coated nanoelectrode was placed adjacent (~2 μm) to the cell, while the cell is patched in whole cell current clamp configuration using a micropipette equipped to measure the plasmonic responses. We used AuNPs of approximately 20 nm diameter, for which the SPR peak is around 520 nm wavelength, and visible light source at 532 nm, to irradiate the AuNPs. The 532 nm green laser (OBIS 532 nm laser, Coherent, Santa Clara, CA) pulses were focused on the tip of the AuNPs-coated nanoelectrode through an optical fiber with a 50 μm inside diameter (custom fiber optic cannula from ThorLabs). The effects of the Au nanoparticles are explained in more detail in the Discussion section.

Electrical evoked action potentials were measured pre and post optical stimulation, also pre and post hybrid stimulation. Plasmonically evoked APs were recorded in response to laser stimulation with a 50 μm diameter optical fiber (green, 532 nm, 1-5 ms pulses, 50-300 ms overall duration of repetitions, 10 pulses/s). For hybrid stimulation, sub-threshold electrical stimulus was added in addition to the optical stimulus. Cellular response was recorded using the patch-clamp system in whole-cell current-clamp configuration mode. Figure 8 shows the micrographs of one such plasmonic, i.e. hybrid, stimulation experimental setup used for neural cell action potential recordings.

In current-clamp mode, the holding membrane potential was maintained at −60 to −70 mV. Threshold (TH, the most hyperpolarized potential at which the cell was able to fire an AP) was determined by injecting increments of depolarizing current (Δ of 50-100 pA) for 5 ms pulse width, until the cell started to elicit AP.

For the plasmonic stimulation, electrical stimulus was switched off, and cells were excited by the output of a 137 mW laser using green light (532 nm visible wavelength) pulsed by

a monofilament laser fiber, aimed at the tip of a gold nanoparticle-coated micropipette positioned next (~2 μm) to a patched trigeminal cell.

For the hybrid stimulation, electrical stimulus was added back, in addition to the optical plasmonic stimulation, at a reduced sub-threshold (30-40% less) current input (pA) from the previously determined threshold value. The observed threshold level for trigeminal neurons was 300 pA, as shown in Figure 10, above. Electrical action potentials were measured pre and post plasmonic and pre and post hybrid stimulation.

Note that this setup and approach of hybrid stimulation may work for modulating action potentials of cardiomyocytes, which was previously demonstrated by our group as feasible with optical stimulation alone.

4. Results

4.1. Characterization of Au NPs

4.1.1. UV-Vis Spectral Analysis of colloidal AuNPs solution

The AuNPs absorption properties of visible light are responsible for the manifestation of the LSPR phenomena. An ultraviolet-visible (UV/Vis) spectroscopy method is used to quantify the absorbed and scattered light of a AuNPs containing sample. A visible color change of the gold solution from yellow to reddish maroon was observed during synthesis. A Perkin Elmer Lambda 35 UV/Vis spectrophotometer was used (190-1100nm wavelength range, 0.5-4nm variable bandwidth range) to obtain the UV/Vis absorption spectra of the AuNPs solution. A strong LSPR absorption spectrum was recorded with a maximum peak at the 520 nm wavelength, for our synthesized colloidal Au solution, indicating formation of AuNPs (Figure 8).

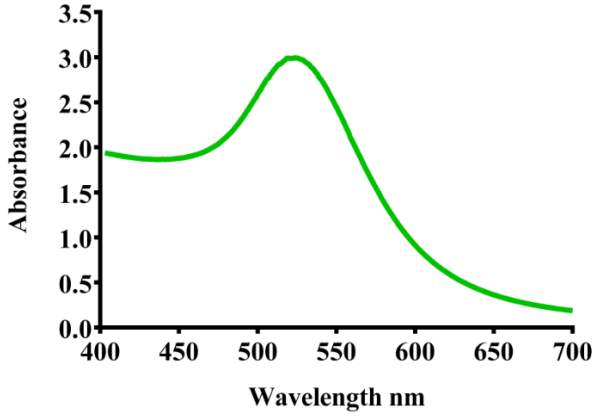

Figure 11. LSPR absorption spectrum of AuNPs, with a maximum peak around 520 nm.

4.1.2. Particle size distribution

The particle size distribution was characterized using a Malvern Zetasizer Nano Series instrument, which works on the principle of light scattering to measure the particle size distribution. Using a disposable pipette, the Zeta cell is filled with the Au nanoparticles sample solution (~ 1.5 ml). When full, the cell is placed in the sample chamber with the electrodes facing the sides of the system. After the system optimizes the laser attenuation and run time, data collection begins, producing the count rate, the phase plot and the log sheet in real time.

The particle size distribution curve and histogram by number (percent) of the synthesized AuNPs, determined using the Zetasizer particle counter, show the AuNPs are in the range of 10-20 nm size diameter, displaying normal distribution in that range.

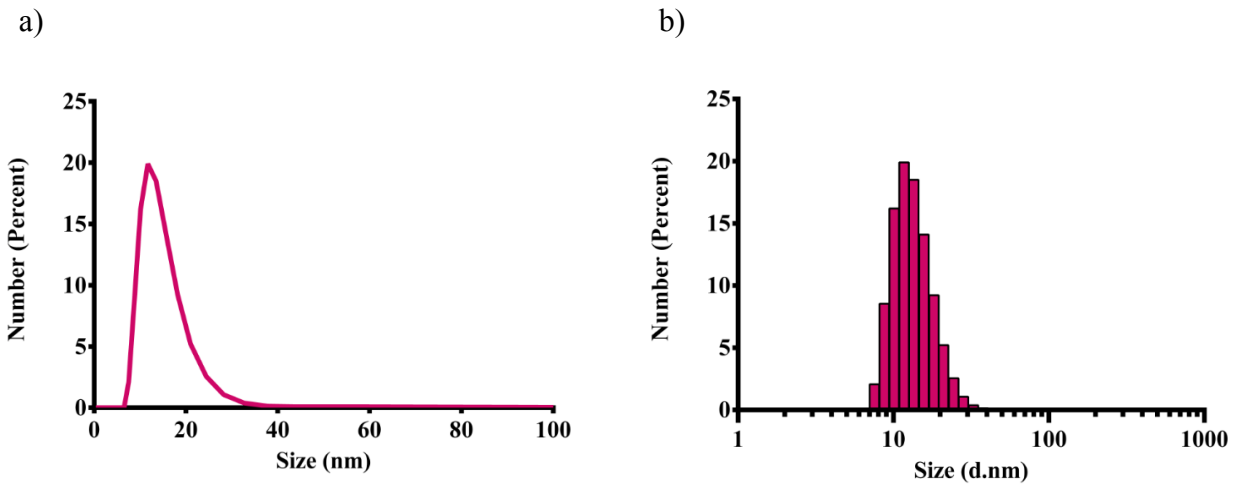

Figure 12. AuNP Solution Particle Size Characterization. (a) Particle size distribution curve, showing a normal distribution centered around the 10-20 nm particle size diameter. (b) Histogram for particle size distribution data by number (percent) of the synthesized AuNPs particle size diameter, determined using Zetasizer particle counter. The histogram buckets confirm a normal distribution centered around the 10-20 nm particle size diameter.

4.1.3. TEM Imaging of the colloidal gold solution

Images of the gold nanoparticles were obtained using an FEI Morgagni transmission electron microscope (TEM), based on transmitted electrons through the thin layer of a sample. Figure 10 shows two TEM two dimensional images of the gold nanoparticles: at a 50 nm scale bar and at a 20 nm scale bar. The colloidal AuNP diameters displayed a normal distribution around 10-20 nm, as shown in the images below.

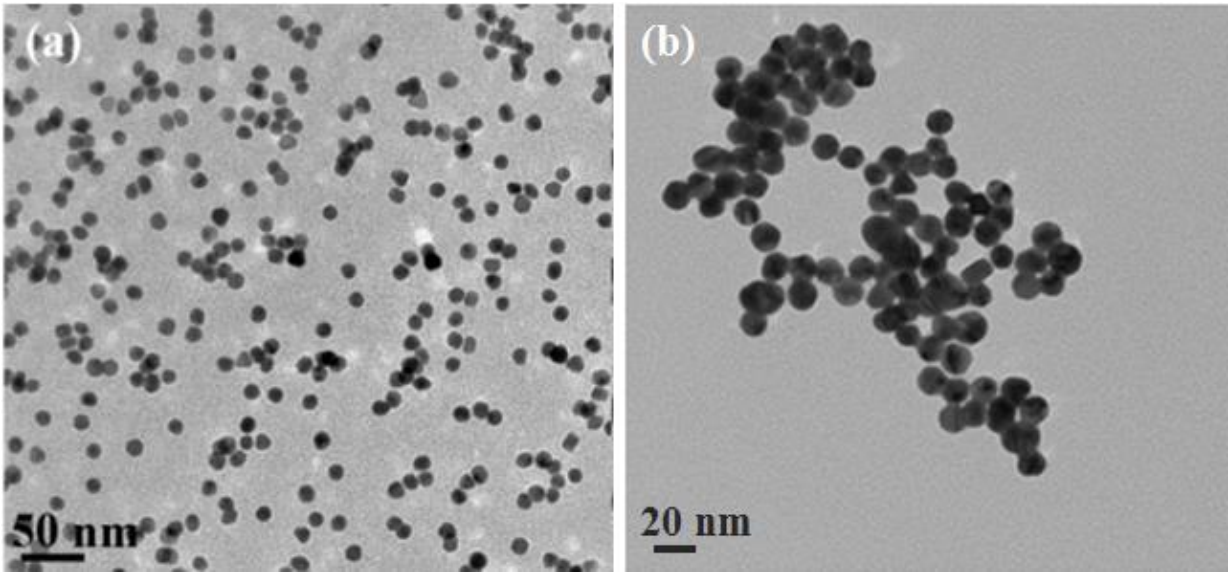

Figure 13. TEM image of the AuNPs suspension, which was synthesized using a liquid phase method by adding 2-3 ml of a 1% solution of trisodium citrate to a boiling $HAuCl_4.3H_2O$ solution, under continuous stirring, and boiled until it turned maroon red in color, indicating the presence of AuNPs, at different magnification. Some agglomerates may be present in these TEM images, although dispersed over the entire sample observation volume subject to imaging. At the 20 nm individual particle size distribution level, these agglomerates are sonicated just before dipping the pipettes in order to form a self-arranged coating layer through the dip coating technique.

4.1.4. SEM Imaging of the AuNPs coated Nanoelectrode

The coating uniformity of the AuNPs on the borosilicate glass surface was verified using scanning electron microscopy (SEM) imaging, obtained with a Hitachi SU70 scanning electron microscope, focusing on the nanoelectrode surface. Figure 14 shows the SEM images of the gold nanoparticles: at a 10 μm, 3 μm, 2 nm, and 200 nm scale bars. The distal tip of the coated nanoelectrode is the portion that comes closest to the neuron cell.

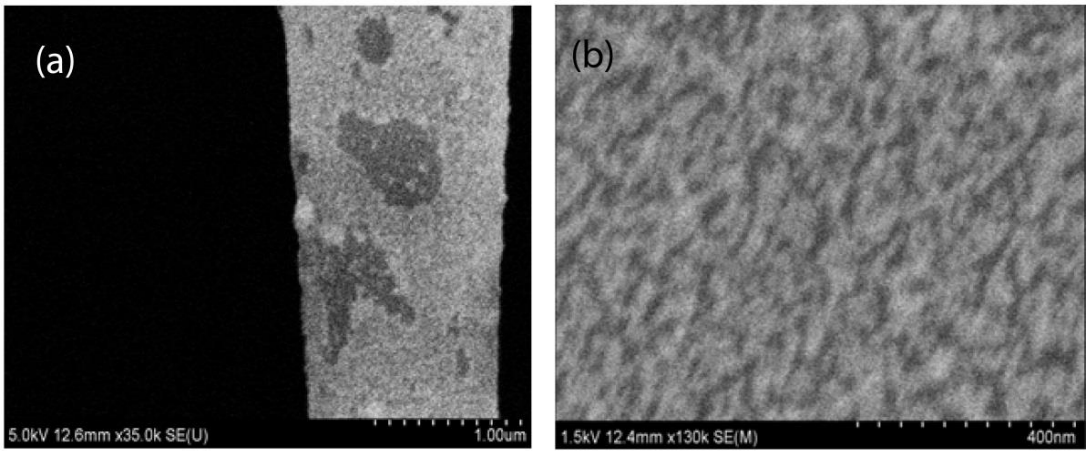

Figure 14. SEM images of the nanoelectrode coated with ~20 nm diameter colloidal gold nanoparticles (AuNPs), at different magnifications: (a) 1 μm; (b) 400 nm scale.

4.2. Plasmonic and Hybrid Physiological Responses

All plasmonic and hybrid stimulation experiments were performed using the patch clamp set up equipped with Multiclamp 700B amplifier and Digidata 1440A data acquisition system (Molecular Devices) depicted in Figure 6. Initial neural stimulation experiments were performed to establish a baseline for LSPR-enabled plasmonic stimulation thresholds. All electrophysiological experiments were done in a whole-cell patch-clamp configuration.

The individual trigeminal neurons were patch-clamped in the standard whole-cell current clamp configuration using a patch-clamp electrode and then transiently exposed to a 532 nm laser pulse (75-125 mW power, 1-5 ms pulse duration) aimed at the tip of a AuNPs-coated micropipette positioned next (~2 µm) to the patched trigeminal neuron cell (Figure 8). A 50 µm inside diameter optical fiber was used to focus the 532 nm green laser light on the surface of the nanoelectrode. Figure 8 shows the electrode setup in the petri dish, when the laser beam shines upon the tip of the nanoelectrode producing the plasmonic effect.

The holding current was adjusted to the minimum threshold value in order to set the membrane potential to a baseline value (around -70 mV). The trigeminal cells were first stimulated with depolarizing electrical currents to trigger a control AP and verify that cells were electrically excitable before proceeding to plasmonic excitation (Figure 15). The electric current is held constant while the corresponding membrane voltage of the cell is measured.

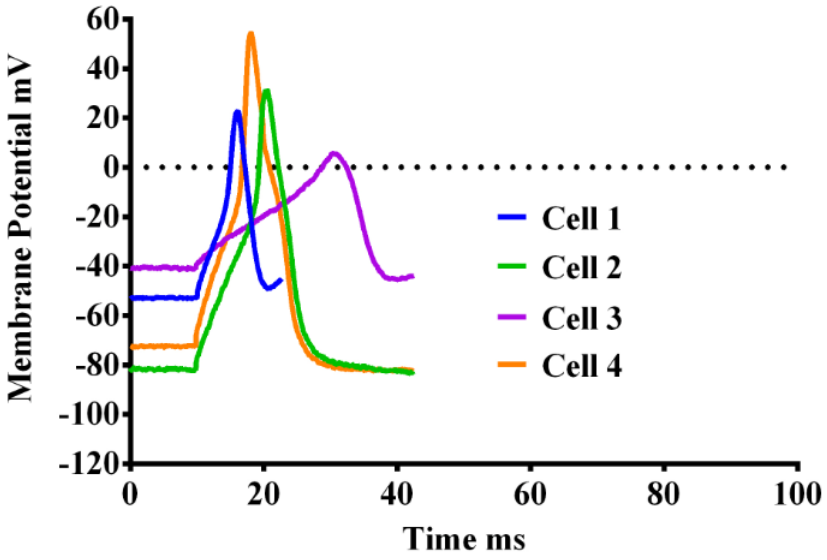

Figure 15. Electrical stimulation APs (pre-plasmonic) recorded from four representative cells when cells were stimulated with electric current pulses (150–300 pA, 300 ms) – control condition.

Then the patch-clamped trigeminal neuron was stimulated with visible 532 nm light delivered from an optical fiber at 75-125 mW laser power for 1-5 ms duration, by shining the laser beam at the tip of a AuNPs-coated micropipette positioned next (~2 μm) to the patched neuron. The presence of the AuNPs-coated nanoelectrode, in the close vicinity of the neurons, enabled responses to the applied 75-125 mW, 1-5 ms laser pulses, although with limited success due to the heat-only oriented stimulation input when using just the optical stimuli. A fraction of the stimulated cells (4 out of 23) produced AP responses with pure optical stimulation, while the rest of the cells responded with only a shift in membrane potential or an incomplete/partial repolarization only. Representative traces of the current-clamped trigeminal neurons (N=4), firing action potentials in response to the plasmonic stimulation are presented in Figure 16.

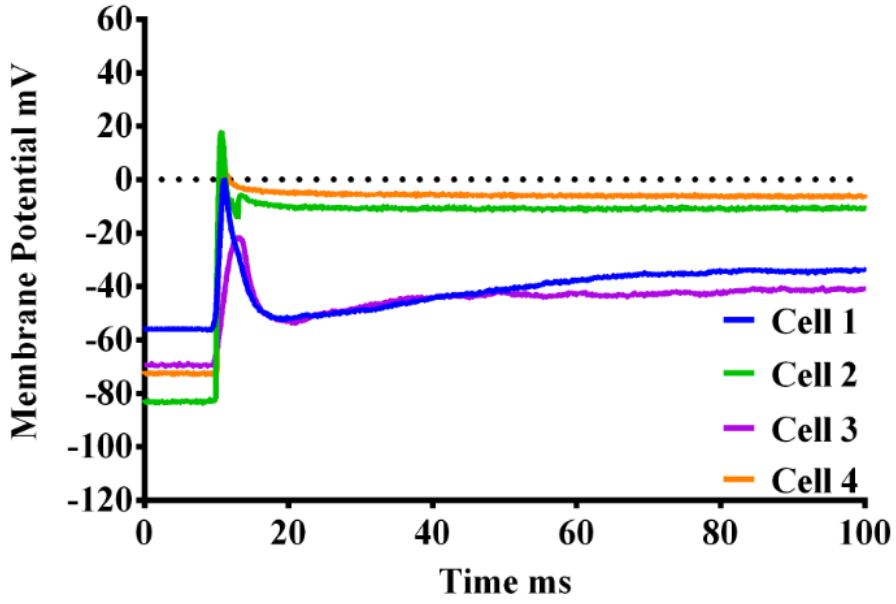

Figure 16. Four representative cells excited by plasmonic neural stimulation. Plasmonic stimulation APs were recorded when cells were stimulated for 1-5 ms by green laser pulses (75-120 mW laser power) starting at time 10 ms in the observation interval on the x-axis. The pure optical (plasmonic) APs were smaller in magnitude compared to the pure electrical APs (pre-plasmonic), with Cell's 2 and 4 repolarization responses prematurely terminated or inhibited.

It was observed that the pure optical (plasmonic) APs were smaller in magnitude compared to the pure electrical (pre-plasmonic) APs. Also, it was noticeable that the post-plasmonic APs (Figure 17), recorded when cells were stimulated with electric current pulses of the same magnitude (150 pA, 300 ms) as in the pre-plasmonic electrical stimulation (Figure 15), resulted in APs with significantly smaller amplitude than the original electrical APs. Also, one of the four cells did not survive the plasmonic stimulation; therefore, it could not produce a post-plasmonic electrical AP response (Figure 17). Plasmonic action potentials were not consistent, in terms of amplitude and timing, unlike the electrically-induced pre-plasmonic APs.

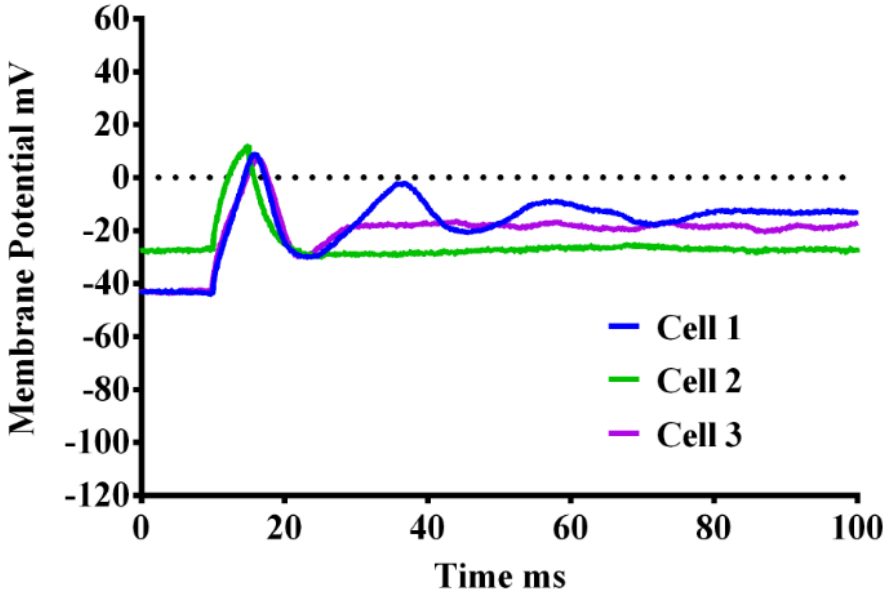

Figure 17. Electrical stimulation APs (post-plasmonic) recorded for four representative cells when stimulated with electric current pulses of the same magnitude as in the pre-plasmonic electrical stimulation (min 150–300 pA, 300 ms). These post-plasmonic APs were recorded with significantly smaller amplitudes than the pre-plasmonic APs. One of the cells did not survive the plasmonic stimulation due to cell damage caused by the optical stimulation, as reported previously, therefore it could not produce a post-plasmonic electrical AP.

While laser light between 75-125 mW power was sufficient to reliably trigger APs, two distinct characteristic types of membrane potential outputs were observed.

Type 1 was the most prevailing characteristic output when the trigeminal neuron cell depolarizes, with no/negligible repolarization of APs following optical laser plasmonic stimulation (Figure 18), indicating possible inhibition. Approximately 80% of plasmonic stimulation attempts (8 out of 10 cells) result in this type of AP response. This was likely related to cell membrane damage due to plasmonic exposure, manifested in the premature termination or leveling out of the AP response into a termination peak immediately after the depolarization phase, with no evident repolarization. In those terminated cells, the post-plasmonic electrical stimulation AP response was often not possible, as the cell's membrane damage led to no physiological response.

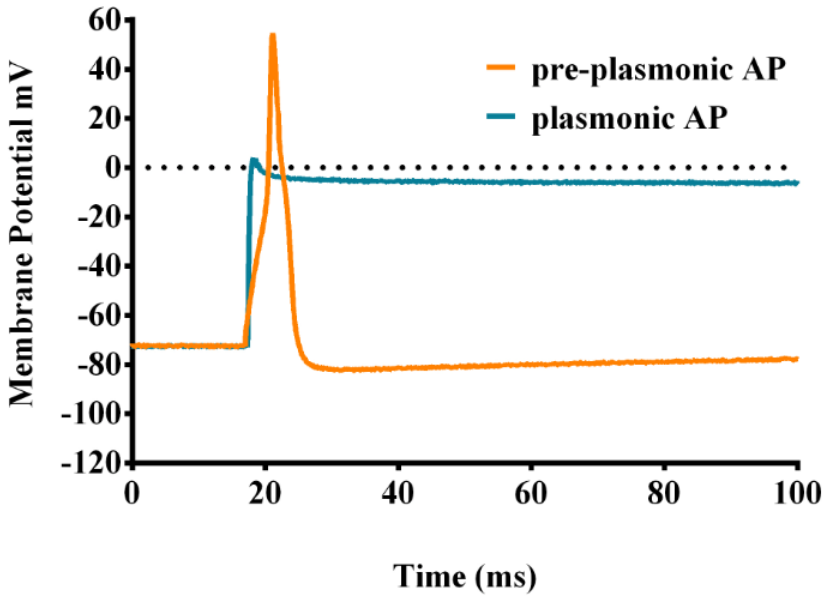

Figure 18. Type 1: Typical plasmonic stimulation AP response of trigeminal neurons in a whole-cell current-clamp recording where the optical AP response is seemingly inhibited and the cell is irresponsive to electrical stimulation post-plasmonic optical stimulation.

This outcome implies cell membrane damage, or inhibition similar to passivation, resulting in ion channel dysfunction, which plays a principal role in regulating cellular excitability and whose damage or misbalance can cause irregular depolarization and repolarization patterns. This is manifested in the premature termination or leveling out of the AP response peak, immediately after firing the plasmonic-triggered AP discharge, with no/minimal evident repolarization down-slope once reaching the peak. In some of those cells, the post-plasmonic electrically-evoked AP response returned to normal, after a short resting period (few seconds to minutes). In some cases though, the post-plasmonic electrical stimulation was not possible, as the cell membrane demonstrated persistently prolonged passive behavior after the optically-induced AP from pure plasmonic stimulation. Similar behavior was reported by researchers who studied effects of AuNPs-aided stimulation of DRG neurons following a laser pulse, indicating cell damage was frequently observed following an AP, resulting in loss of excitability.[4]

Type 2 was the second most typical plasmonic stimulation AP response of trigeminal neurons in a whole-cell current-clamp recording, where the cell was only partially responsive to optical stimulation, producing only a very weak membrane potential shift (10-20 mV jump), therefore not a complete AP, or the cell was completely irresponsive to the plasmonic stimulus following a successful pre-plasmonic electrical stimulation AP (Figure 19). This can be partially dependent on the nanoelectrode positioning and proximity to the cell (nanoelectrode tip must be next to the cell, <2 μm distance) and laser beam clearly focused on the tip of the nanoelectrode to get sufficient thermal effect for the LSPR in order to produce plasmonic excitation results, in addition to the magnitude of laser power used. The positioning of the nanoelectrode was visually controlled in the petri dish through the 40 x magnification eyepieces with reticle.

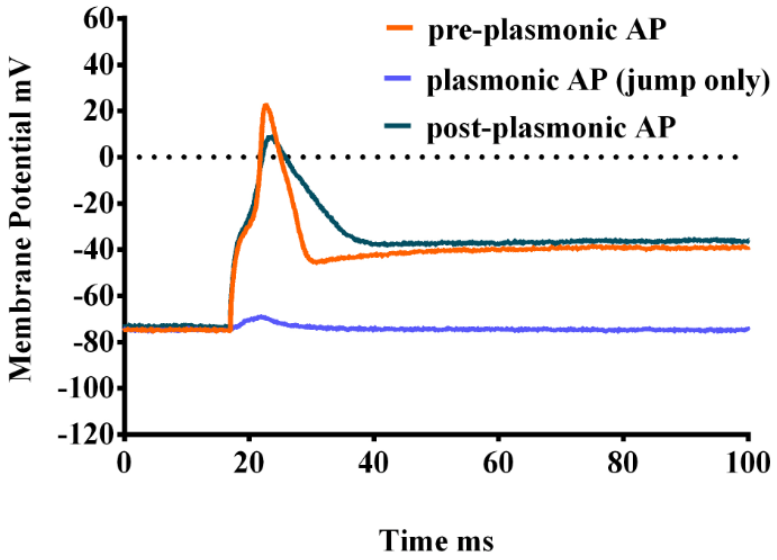

Figure 19. Type 2: Typical plasmonic stimulation AP response of trigeminal primary neurons in a whole-cell current-clamp recording where the cell is only partially responsive to optical stimulation with no full AP depolarization (only a weak shift, ~20mV jump), following a successful pre-plasmonic electrical stimulation AP firing. In those irresponsive cells, the post-plasmonic electrical stimulation AP response had slightly smaller amplitude, compared to the pre-plasmonic electrical stimulation AP response, and it lacked repolarization acuity.

It was observed that laser power of < 75 mW directed at the surface of the AuNPs coated nanoelectrode was insufficient to stimulate the cells. Laser power between 75 – 125 mW was sufficient to generate the plasmonic effect and evoke AP response in the trigeminal neurons. Approximately 20% of plasmonic stimulation attempts (2 out of 10 cells) resulted in Type 2 profile of a suppressed membrane potential response when subjected to plasmonic stimulation. Although these Type 2 cells recover sufficiently and are able to fire full AP in response to a post-plasmonic electrical stimulation, they do lack repolarization acuity, indicating the suppression has detrimental effect, where a diminished repolarization becomes noticeable when the cells are electrically stimulated post-plasmonic stimulation. This indicates temporary impairment or permanent irreversible damage of the cell membrane caused by the pure plasmonic stimulation.

This side effect is consistent with literature, in that plasmonic stimulation results in a reluctance of the cell to recover quickly and fully to its original base state in a short amount of time once the heat is discontinued.[4, 46] We observed the recovery time for the membrane to return to its original pre-plasmonic excitability or resting potential state to be a few seconds to a minute. This could be due to an increased tendency for cellular damage as a consequence of the local photothermal effects, due to high-efficiency light energy accumulation around the gold-nanoparticle-conjugates or the gold-nanoparticle-coated nano-surfaces when nanoparticles form larger clusters. This can be an area for further studies to quantify how multiple layers and spatial arrangement of nanoparticles affect the amount of heat generated in the cell's immediate vicinity, and to further characterize and optimize the configuration and uniformity of the nanoparticle-conjugates and coated interfaces to be tailored for optimal neural stimulation.

To address the shortcomings of pure optical stimulation, we hypothesized that combination of short-duration optical with sub-threshold levels electrical stimulation will avoid damaging the cells. Hence, next, we employed a combined electrical and optical stimulation procedure to utilize the advantages of both stimulation modes, and to introduce the ability to turn on and off individual neurons by fine tuning the proposed hybrid stimulation (combined optical and electrical). We also optimized the neural outputs with various combinations of short duration repetitive bursts of electro-plasmonic pulses to modulate neural firing patterns. These results provide proof of concept for using this type of hybrid electro-plasmonic stimulation to elicit APs.

Representative traces of the current-clamped trigeminal neurons show firing APs in response to the hybrid stimulation, when cells were stimulated with the combined 1-5 ms, 532 nm green laser pulses and a sub-threshold electrical current pulses at reduced levels (Figure 21). The recorded hybrid stimulation APs, when short duration laser pulses (1-5 ms) were combined

with electric current pulses, were comparable in magnitude as well as timing to the pure electrical (pre-hybrid) APs (Figure 20). Further, the peak responses recorded with hybrid stimulation were higher than the previously recorded peak responses with pure optical stimulation alone, by 10 to 20 mV.

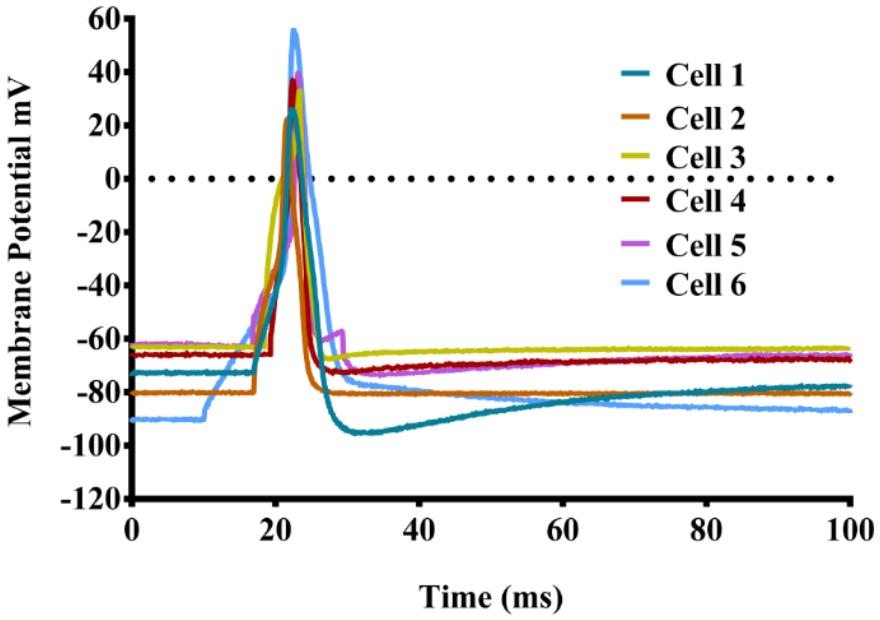

Figure 20. Pre-hybrid electrical stimulation APs recorded when cells were stimulated with electric current pulses (150 – 300 pA, 5 ms) – control condition.

When short-duration laser pulses (1-5 ms) were superimposed with electric current pulses for a hybrid electro-plasmonic stimulation, membrane APs were reliably recorded from trigeminal neurons. Peak responses recorded with hybrid stimulation (Figure 21) were higher than pure optical stimulation (Figure 16) by 10 to 20 mV on an average. In addition, the post-hybrid APs (Figure 22), recorded when cells were stimulated with electric current pulses of the same magnitude (150 – 300 pA, 5 ms) as in the initial pre-hybrid electrical stimulation (Figure 20), resulted in APs with comparable amplitude to the original (pre-hybrid) electrical APs.

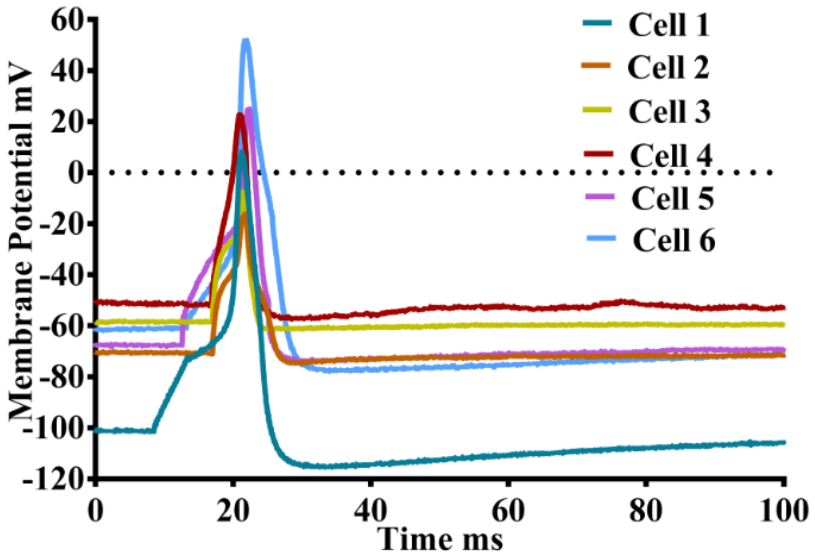

Figure 21. Hybrid electro-plasmonic stimulation APs recorded when cells (N=6) were stimulated with the combined 1-5 ms, 532 nm green laser pulses (75-120 mW laser power) and sub-threshold electric current pulses at ~ 40% reduced levels from the (300 pA) threshold values.

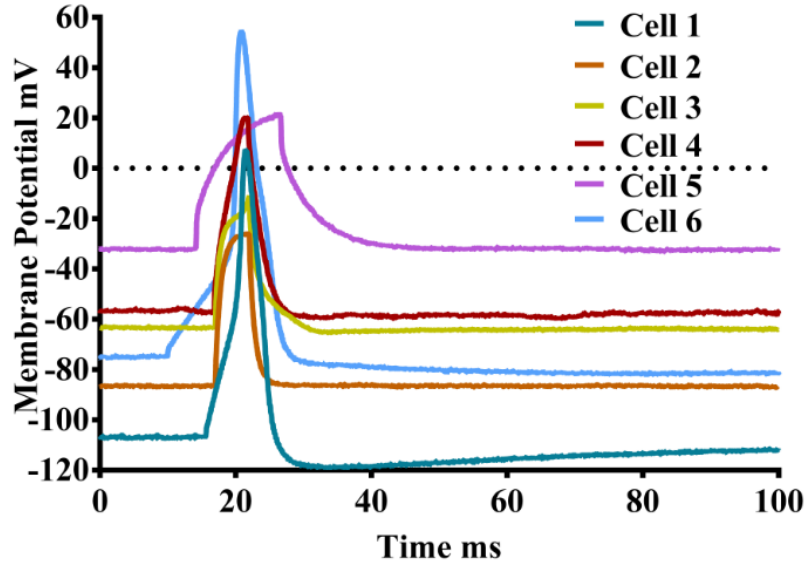

Figure 22. Post-hybrid electrical stimulation recordings when cells were stimulated with electric current pulses of the same magnitude as in pre-hybrid stimulation (150 – 300 pA, 5 ms) – control condition. Cells made consistently similar AP responses as the original values observed from the initial electrical (pre-hybrid) stimulation.

Also, all cells survived the hybrid stimulation and did produce post-hybrid electrical stimulation APs (Figure 22), unlike post plasmonic stimulation (Figure 17). This survival rate was higher as compared to after pure plasmonic stimulation, most likely because there was no indication of membrane damage. It is likely that pairing the short-duration green light pulse stimulus with electrical current pulses aids the electrically excitable ion-gate activation in addition to the plasmonically triggered photothermal activation effects. So, these two stimuli have mutually some beneficial additive effects on the resulting AP responses.

The mean plasmonic AP responses (Figure 23 a) and the mean hybrid (electro-plasmonic) AP responses (Figure 23 b) were further compared for variation and profiling.

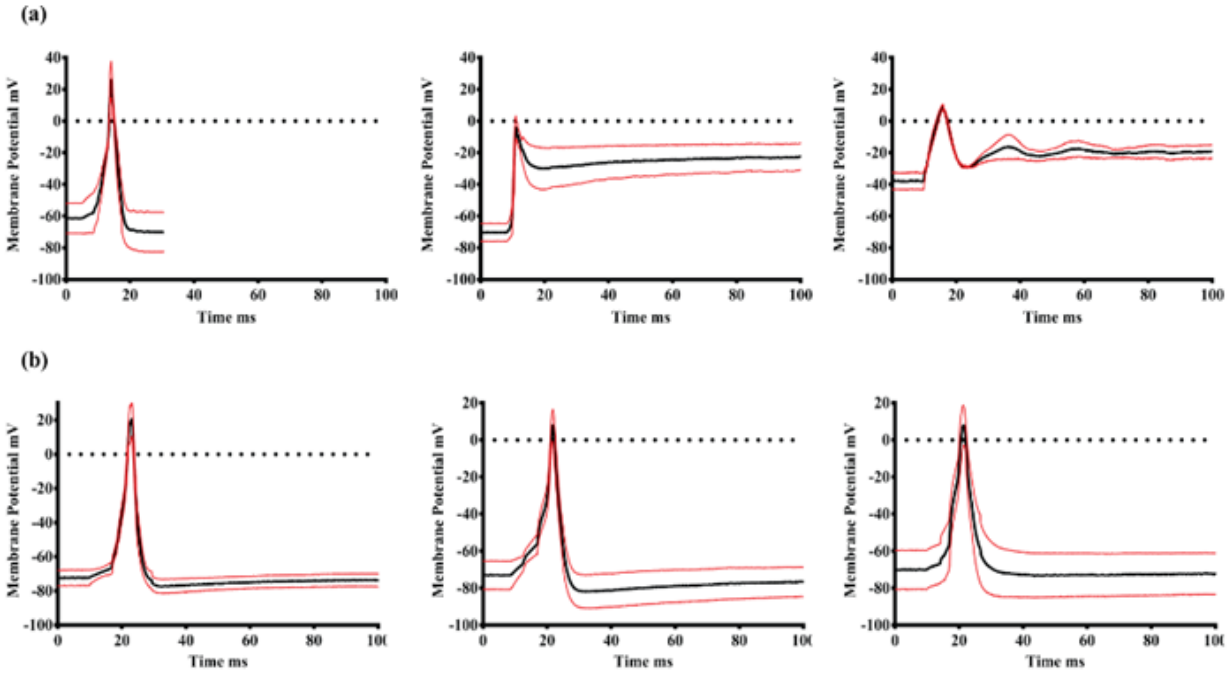

Figure 23. Comparison of Plasmonic vs. Hybrid stimulation results of primary mouse trigeminal neurons - Whole Cell Current Clamp Recordings. a) Mean plasmonic electrophysiology AP responses (N=4). Left: Pre-plasmonic electrical AP responses. Middle: Plasmonic APs response. Right: Post-plasmonic electrical APs response. b) Mean hybrid (electro-plasmonic) AP responses (N=6). Left: Pre-hybrid electrical AP responses. Middle: Hybrid (electrical + optical) AP responses. Right: Post-hybrid electrical AP responses.

In hybrid stimulation, the electrical stimulus input current required to evoke APs was reduced by 33 - 38% when a plasmonic stimulus (1-5 ms pulse width) was added to the electrical input, as compared to pure electrical current stimulation without the addition of optical stimuli (Figure 24).

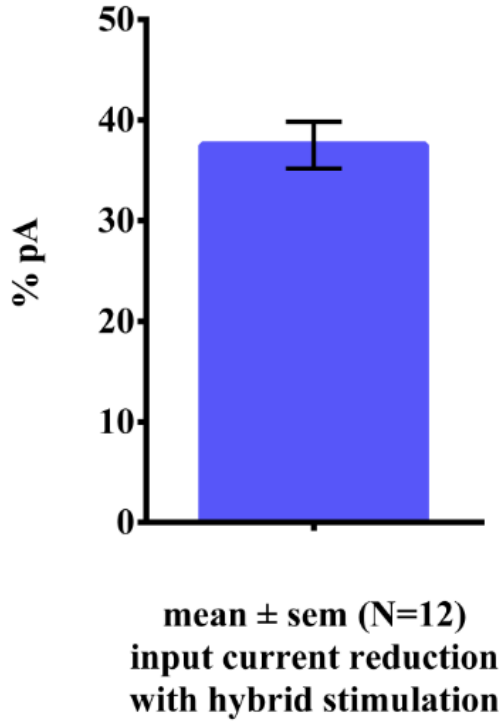

Figure 24. Mean input current reduction (% pA) as observed in (N=12) trigeminal cells when stimulated with hybrid electro-plasmonic stimulation vs. pure electrical current stimulation. The current reduction mean is 38 ± sem.

We also observed that this hybrid neural stimulation has no deleterious effects on the neurons, i.e., the cells fired electrical stimulated APs immediately after the hybrid stimulation, unlike the pure optical stimulation approach alone (as reported above). The observed plasmonic vs. hybrid stimulation AP success rates were 26% (N=23) for plasmonic vs. 83% (N=29) for

hybrid stimulation of the trigeminal neurons. So, 3x the success rate when stimulating with hybrid stimulation vs. plasmonic (Figure 25).

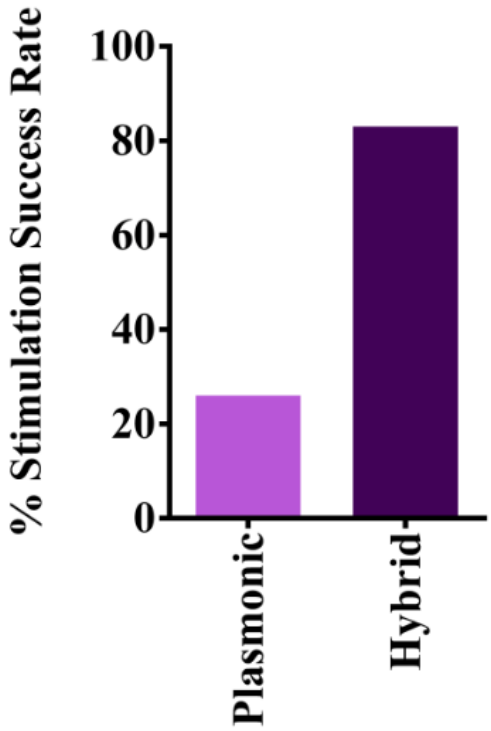

Figure 25. Plasmonic vs. hybrid stimulation success rate. Success rate defined as ratio of number of successful pure optical (or hybrid) stimulation APs vs. the total number of cells stimulated with optical (or hybrid) stimulation respectively. Observed AP success rates were 26% (N=23) for plasmonic vs. 83% (N=29) for hybrid stimulation, for cells that previously produced electrically stimulated baseline APs. The hybrid stimulation success rate is an order of magnitude >3 as compared to the plasmonic stimulation success rate.

The observed plasmonic vs. hybrid survival rates were 13% (N=23) post-plasmonic, vs. 72% (N=29) of trigeminal neurons post-hybrid APs. Therefore, an order of magnitude >5.5x for survival rate of trigeminal neurons when stimulated with hybrid stimulation compared to plasmonic alone (Figure 26).

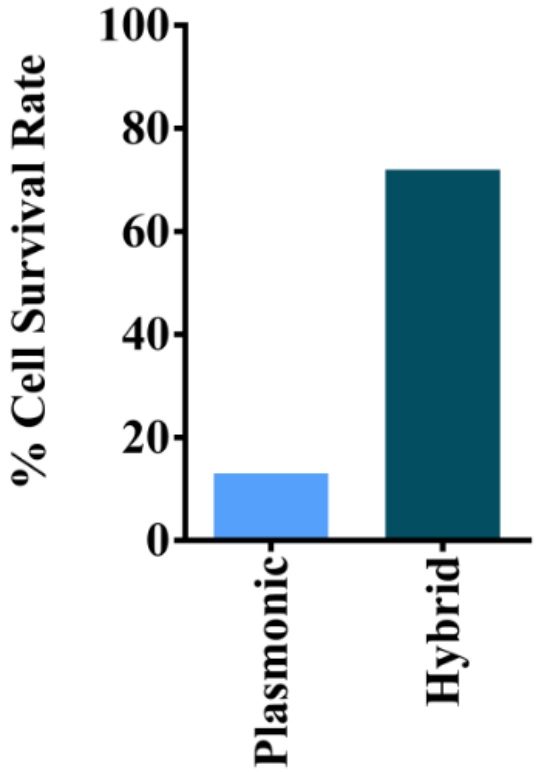

Figure 26. Plasmonic vs. hybrid survival rate. Observed neuron survival rates were 13% (N=23) of trigeminal neurons after plasmonic stimulation vs. 72% (N=29) of trigeminal neurons after hybrid stimulation. The hybrid stimulated trigeminal neurons' survival rate is an order of magnitude >5.5 compared to the plasmonic stimulated trigeminal neurons survival rate.

It was observed that cells died more often when stimulated with pure plasmonic stimulation due to membrane damage as previously reported by our group.[46] It was also observed that hybrid stimulation produced favorable results without obvious cell damage, i.e. fewer cells died, possible explanation is loss of whole cell configuration in those fewer cells that died.

The compound benefits from using hybrid vs. pure plasmonic stimulation are obvious (Figure 27). The side-by-side comparison overview of the success rate and the survival rate for

each type of stimulation mode clearly shows the dual benefit from using hybrid over plasmonic stimulation alone.

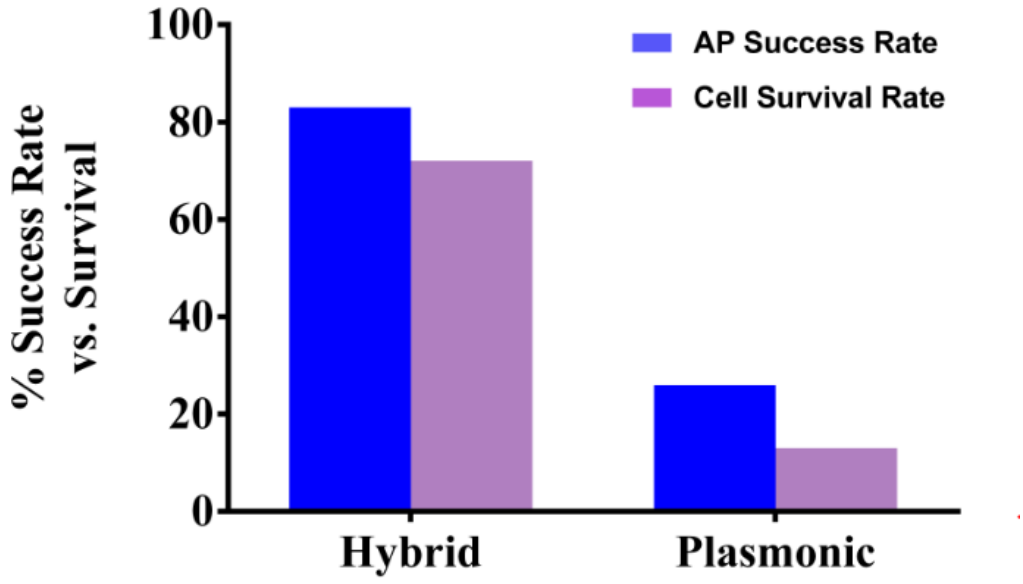

Figure 27. Side-by-side comparison overview of the dual benefit, better success rate and survival rate, of using hybrid stimulation vs. pure plasmonic stimulation mode. For hybrid stimulation the observed AP success rate was 83% and the observed neuron survival rate was 72% (N=29). Plasmonic stimulation outcomes were 3-5 times more inferior overall, compared to hybrid, with observed AP success rate of 26% and observed neuron survival rate of 13% (N=23).

Further optimization experiments were carried out to study the lead- and lag-time effects of electrical vs. plasmonic pulses in a hybrid electro-plasmonic stimulation combination on AP generation. Electro-plasmonic hybrid stimulation (5 ms; 75-120 mW, 532 nm, 5 ms) pulses were presented to trigeminal neurons at sub-threshold electrical input currents. We found that a lead or lag time greater than 1.4 ms, of either electrical or optical pulse in reference to each other, did not produce proper standard neural stimulation APs; there was only a shift in membrane

potentials. Optical lead times of up to 0.6 ms before electrical pulses produced standard APs. Electrical lead times of as low as 0.4 ms before optical, and up to 1.4 ms before optical also produced good hybrid APs (Figure 28).

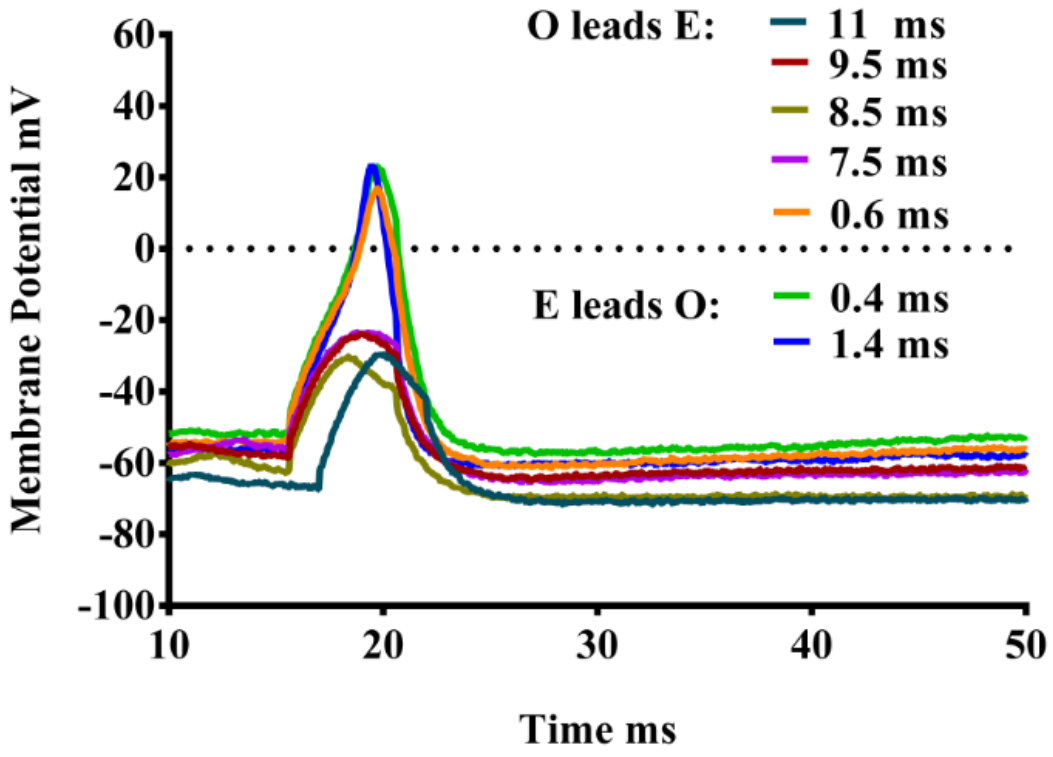

Figure 28. Lead and lag time optimization of hybrid stimulation opto-electric parameters. Lead and lag time optimization of hybrid stimulation opto-electric parameters. The effects of electrical vs. plasmonic pulses lead and lag time on our hybrid electro-plasmonic stimulation paradigm: Electro-plasmonic hybrid stimulation (5 ms; 75-120 mW, 532 nm, 5 ms) pulses were applied at a sub-threshold electrical input current. The shift in membrane potential indicates that a lead or lag time greater than 1.4 ms, of either electrical or optical pulse in reference to each other, did not produce proper AP responses. Optical lead of up to 0.6 ms before electrical, as well as electrical lead of up to 1.4 ms before optical, both produced good hybrid APs.

We concluded, based on the above, that electrical pulse leads of <1 ms before optical was the best condition to excite neurons. In additional experiments, the optical pulse duration (1ms) was fixed and the electrical pulse duration was varied, from 1 to 5 ms, at the hybrid sub-threshold intensity level, where the electrical pulse preceded the optical by 0.7 ms. AP peak responses increased as the sub-threshold electrical pulse duration increased, as shown in a representative hybrid stimulation of a primary trigeminal neuron, where electrical pulse durations between 3-5 ms produced optimal AP response (Figure 29).

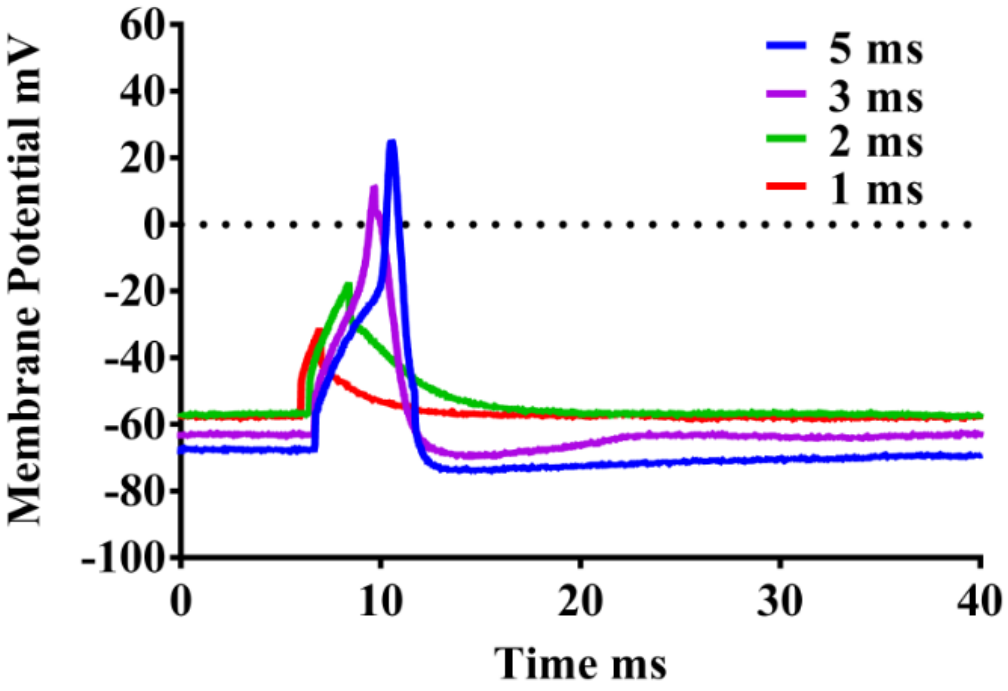

Figure 29. Optimization of hybrid stimulation pulse duration for best electro-plasmonic stimuli. At a fixed optical pulse duration (1ms), hybrid sub-threshold electrical stimulation was varied from 1 to 5 ms, where the electrical pulse leads the optical by 0.7 ms in time of initiation. AP peak responses increased as the sub-threshold electrical pulse duration increased, with pulse duration of 3-5 ms being the optimal for getting full AP response from the neuron.

The difference (delta) between the AP peak value and base value (first minimum after peak) increased with pulse duration increase, due to the increase in the AP peak maxima as well as the increase in the hyperpolarization, resulting in full AP responses as the pulse duration reached between 3–5 ms. Below 3 ms electrical pulse duration, there was no proper AP response.

Our findings further show the applicability of short duration pulses (1-5 ms) when applied repeatedly, for sub-threshold electrical and LSPR visible light stimulation (Figure 30).

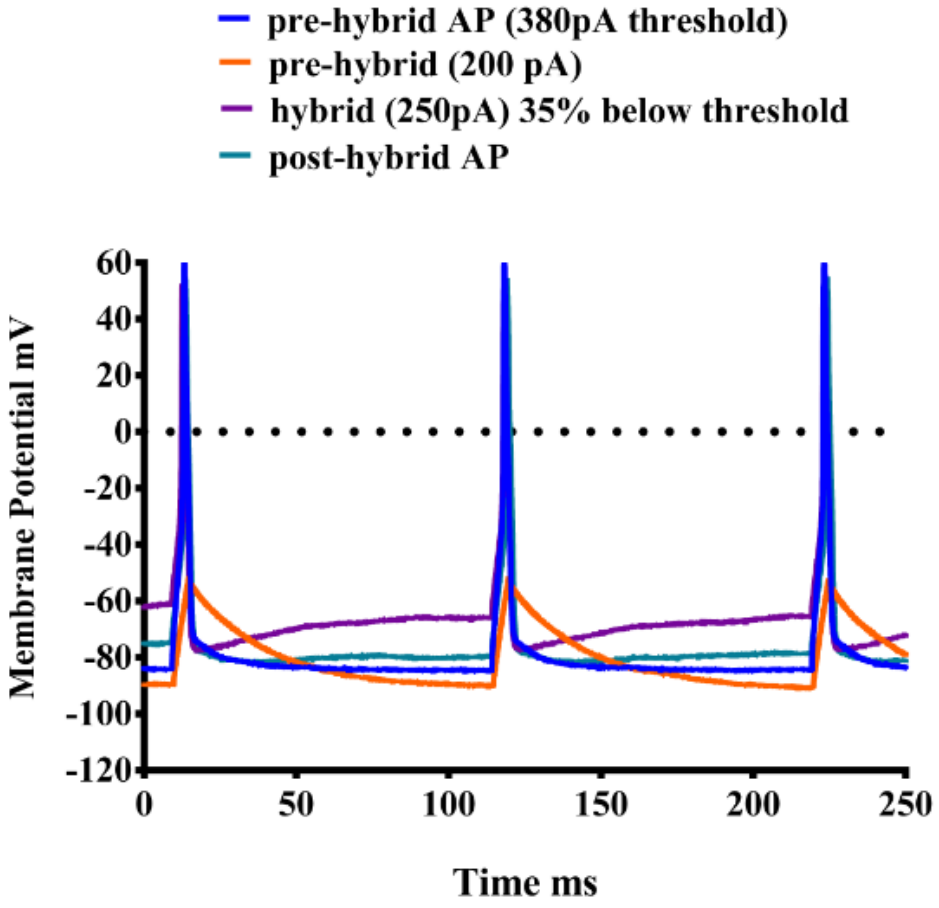

Figure 30. Multiple APs recorded for hybrid electro-plasmonic stimulation. The reduction of current required to trigger APs with the repeated hybrid stimulation was still up to ~40%, as previously shown in Figure 24, and cells stayed healthy longer after repeated exposure to hybrid stimulation compared to pure plasmonic stimulation.

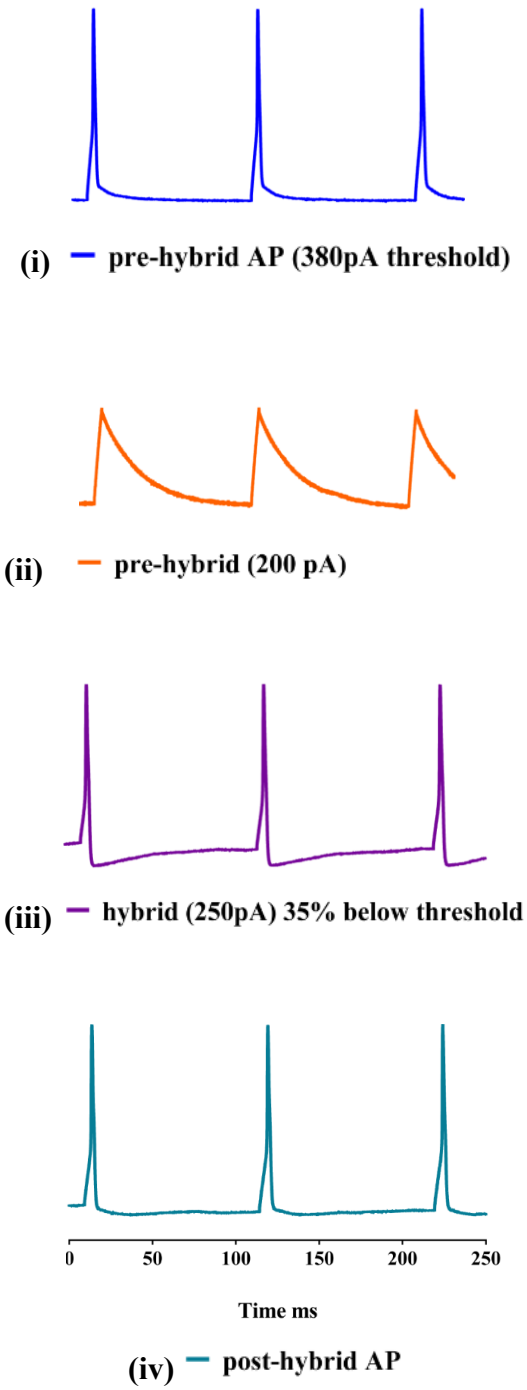

Figure 31. Insets of multiple hybrid stimulation APs, from previous Figure 30, show the separate traces of multiple APs individually for better visibility: (i) Pre-hybrid electrically evoked multiple APs (this cell: 380 pA threshold); (ii) Pre-hybrid electrically evoked shifts (200 pA); (iii) Hybrid stimulation APs (250 pA, 35% below threshold); (iv) Post-hybrid electrically evoked APs.

Our findings show the applicability of short duration pulses (1-5 ms) when applied repeatedly, for sub-threshold electrical and LSPR visible light stimulation pulses, in combination with AuNPs-coated substrates (nanoelectrodes), for obtaining repeatable multiple trains of APs from neurons (Figure 30). Neural cell survival rates and viability after hybrid stimulation was superior to that of pure optical stimulation. The input current sufficient to trigger APs with multiple hybrid stimulation was 35-40% lower, matching what was observed earlier with single AP recordings. This reinforces the previous findings above, supporting the effectiveness of the proposed platform for hybrid electro-plasmonic stimulation of neurons.

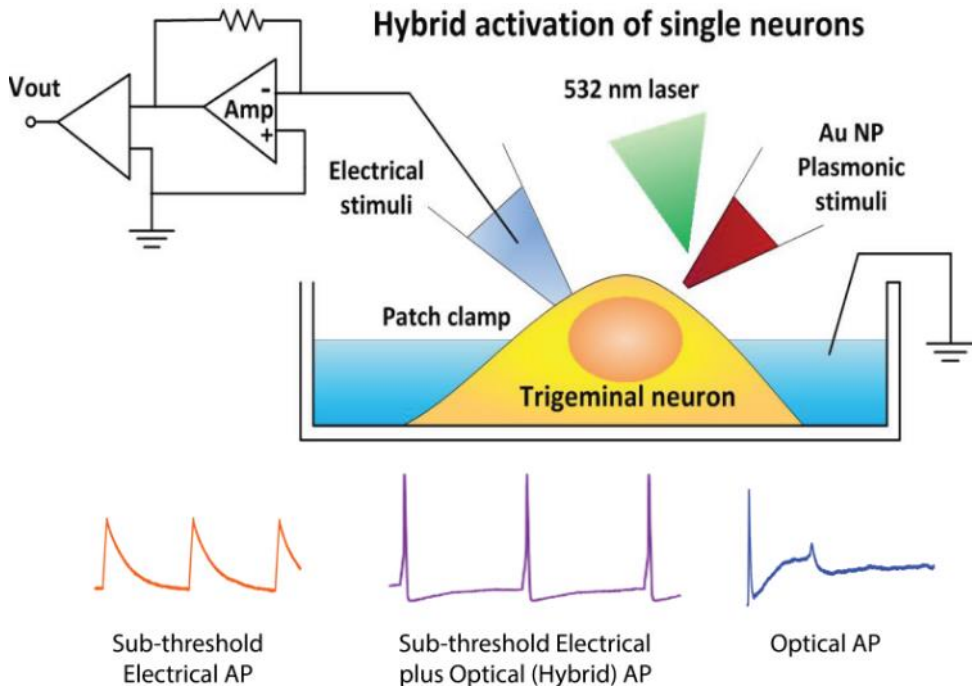

Figure 32. Schematic representation of the hybrid stimulation setup for measurement of neuronal APs produced by multiple electro-plasmonic stimulation. It shows the output traces from the pure sub-threshold electrical (left bottom) and pure short-duration plasmonic (right bottom) stimulation are inferior compared to the hybrid (middle) stimulation output when those two input stimuli are combined together.

5. Discussion

Here, we successfully demonstrated a safe and reproducible hybrid laser stimulation of primary trigeminal neurons using single and multiple pulses of visible light and electric currents. This was presented as an optimized new technology platform for a hybrid electro-plasmonic modulation of neuron excitability using visible-light-sensitive gold nanotransducer particles. Gold nanoparticles (AuNPs) were used to coat the plasmonic stimulation nanoelectrodes, since they are known to demonstrate the desired localized surface plasmon resonance (SPR) effects, and are biocompatible in multiple *in vivo* applications such as drug delivery, bioimaging, biosensors, etc.[62] LSPR fields are generated as a result of the strong surface interactions between the light and the conduction band electrons of the metal nanoparticles. A hybrid modulation neurodevice based on non-contact and non-modification of neural interface approaches, using wireless SPR phenomena, is the ultimate solution for achieving enhanced spatial resolution and thus, more clinically useful focal stimulation of neurons, with the additional advantage of not generating excessive electrical artifacts that could interfere with concurrent neurophysiological recordings, currently used in electrical closed-loop neuroprosthetic systems for treating brain disease, hearing loss/deafness, and similar neurological disorders, as well as in experimental neuroscience.

The plasmonic oscillations in most metal nanoparticles occur mainly in the ultraviolet (UV) region. However, in the case of gold (Au), silver (Ag), and copper (Cu) nanoparticles, the plasmons shift nearer to the visible light domain, related to electrons in the s-atomic orbitals. Specifically, for gold nanoparticles, as those used in the present work, the SPR peak is around

520 nm and it can be tuned with particle size and shape. The AuNPs, especially small size particles (<20 nm), are known to generate localized heating[63, 64] due to SPR, called plasmonic heating. We used AuNPs of approximately 20 nm diameter and visible light at 532 nm, near to the maximum position of the LSPR band in gold, to irradiate the AuNPs.[65] It has been demonstrated that photosensitive AuNPs can be excited upon visible light irradiation and used to wirelessly stimulate primary neurons, and more specifically, trigeminal neurons, without any genetic modifications or direct neural membrane surface contact. Compared to the currently predominant photothermal neuromodulation techniques using direct IR laser stimulation, which is susceptible to collateral heating, there is a fundamental difference in transduction. Au nanoparticles are the photoabsorbers, as opposed to water, nearby cells or extracellular fluids, allowing heat distribution to be controlled and localized at sub-micron levels. With this approach, biomedical implants based on SPR phenomena have the potential to give better spatial resolution and thus more clinically useful focal stimulation. A hybrid modality is presented here, which adds small amounts of electric currents for cell stimulation, to overcome the issues with reproducibility, repeatability and reliability as seen with pure optical stimulations. Hybrid significantly reduces the amount of current as compared to pure electrical stimulation (by ~40 %) as well as facilitates the firing of multiple APs below the threshold. Further optimization experiments with different size/shape of gold particles and controlled deposition of layers on different types of nanoelectrodes could reduce current requirements further.

Electro-plasmonic prototypes based on the hybrid neuromodulation modes presented here have the potential to selectively inhibit or stimulate the electrical excitability of unmodified neurons depending on the specific needs. This can be achieved by varying the tunable electrical and optical stimulation input parameters of the individual inputs through fine-tuning and

optimization of the hybrid stimulation parameters (Figure 30). The fine-tuning of the electro-plasmonic stimulation sequence and variables (lead and lag time, intensity thresholds, duration) administered via short-duration (1-5 ms) repetitive pulsing of both electrical and optical stimuli, allowed for triggering repeatable multiple trains of action potential responses from the stimulated neurons, which is necessary for *in-vivo* applications. It seems that short moderate power optical pulses in milliseconds range are necessary for the successful activation of neurons. It is consistent with other studies using nanoparticles. Relatively high power light is employed by different labs in neuron activation studies (0.31 kW used by Carvalho-de-Souza et al.[4] or 1.5 – 5 kW used by Migliori et al.[66]), while relatively moderate power light is employed in inhibition studies (15 mW photothermal stimulation intensity used by Yoo et al.[10], or 57 mW used by Martino et al.[67], or 120 mW used by Bazard et al.[46]). Also, a number of infrared neurostimulation (INS) studies[68] reported that short wave infrared (IR) pulses (few milliseconds) can stimulate neural fibers including retinal[69] and cortical neurons[70, 71], peripheral[19, 72] and cranial nerves[73-78], central auditory system even cardiomyocytes[46] and neuroblastoma cells[46]. It has been reported that INS is mediated by rapid temperature transients induced by surroundings absorption[18, 72, 79] and that such transients can be induced with other types of photo-absorption as well, thus with visible light plasmonic stimulation as used in our study. It has been previously shown that the rapid temperature transients are directly accompanied by changes in cell membrane capacitance and mechanoelectric properties and resulting modulation of ionic membrane currents can lead to cell stimulation[68]. However, most previous optical/laser studies showed inhibition/modulation of spontaneous neural or cardiac activity; rather than excitation. Whereas we show that exciting neurons is quite feasible with the hybrid stimulation approach. Furthermore, studies have been conducted using external photoresponsive materials such as gold nanoparticles, some needing

genetic modification of the targeted cell, as mentioned above. Other approaches where plasma-membrane-targeted gold nanorods (pm-AuNRs) are prepared with a cationic protein/lipid complex to activate the thermosensitive cation channel, TRPV1, in intact neuronal cells have been tried.[20] The latter method provides an optogenetic platform without the need for prior genetic engineering of the target cells. In our study we use AuNPs coated on an external microelectrode which does not need any bio-conjugation or surface modification of the nano-neural interface to achieve the triggering of neural stimulation. Inhibition or activation is controlled by fine tuning the hybrid input stimuli.

6. Conclusion

In summary, we demonstrated that a reduction of up to ~40% of the starting input current threshold can be achieved for triggering APs, and cells stay healthy longer after repeated exposure to our hybrid electro-plasmonic stimulation platform, with a survival rate greater than five times as compared to pure plasmonic/optical stimulation. In addition, the cell's stimulation success rate was three times greater with the hybrid stimulation. We have shown that combining short-duration green visible light optical pulses with the complementary sub-threshold level electric current pulses can reliably trigger a train of action potentials, possibly by activating ion channels in patterns like standard APs. Collectively, the combined hybrid stimulation input produced reliable APs related to more favorable membrane hyperpolarization. Nanomaterials, specifically gold, maximize the utility of thermal stimulation via surface plasmon resonance phenomena. The use of nanotechnology as a medium for photo-thermal stimulation has the potential to make way for non-invasive neural stimulators capable of cell-specific targeting, allowing for improved restoration of sensorimotor functions and removing side effects exhibited with current neuromodulation methods. This approach may also work with stimulation of cardiomyocytes. Nanomaterials-enabled plasmonic stimulation, when paired with sub-threshold electrical stimulation inputs in a tunable hybrid neuromodulation mode, could revolutionize the way neural or cardiac stimulation therapy is performed.

One good example is the cochlear implant technology and its applications, which after more than five decades, still relies on electrical stimulation of the auditory nerves. Some of the latest advances in cochlear technology are based on bimodal solutions involving a cochlear implant and a hearing aid working together to give the patient a more natural hearing experience

than just the traditional hearing aid or cochlear implant used alone.[80, 81] However, this bimodal solution does not address the underlying cause for why cochlear implant users have difficulty hearing speech in background noise and suffer from poor music perception. Our hybrid neurostimulation findings, utilizing visible light for electro-plasmonic stimulation, open doors of opportunities to develop a new generation of high-acuity neural modulation prosthetic devices, tunable for the individual patient's needs, superior to traditional electrical stimulation technologies and newer photothermal or optogenetic technologies which use infrared or NIR light. Specifically, these capabilities can play a key role in the development of cochlear implants that offer improved frequency specificity with more selective, focused and tunable activation of the auditory neurons along the cochlear frequency axis in deaf patients. Our ultimate goal being to use these advances for implementation of more physiologically effective stimulation channels to achieve better encoding of complex sounds in the auditory nerve via improved spatial resolution.

Last but not least, our hybrid stimulation approach would allow the auditory nerve, i.e. spiral ganglion, to get stimulated with lower current levels while improving specificity, success rate and survival rate of the stimulated neurons, thereby increasing battery life of the cochlear implants. The new generation hybrid cochlear implant technology could consist of an array of optical fibers or similar optical conduit media, i.e. a bundle consisting of thin waveguides (~50 x 80 μm cross section area), paired with an existing technology electrical stimulation electrode array (typically a series of tiny metal rings, as currently used by cochlear implant manufacturers) aligned at the distal end of the cochlear implant, to stimulate the hearing nerve. Such prototype concept of a new generation hybrid electro-optical i.e. electro-plasmonic cochlear implant, shall be feasible based on our research findings presented herein. Alongside the existing electrode

array, we propose to add an optical array of waveguide fibers, which would match the number of electrode rings (for instance, 24 waveguides more or less) staggered in such a way that would allow each optical distal end to pair with a metal ring from the electrode array until all optical fiber ends and electrode rings are paired. The important detail being, each optical fiber i.e. waveguide would have an AuNPs coating applied or built in at the distal end, which would be positioned to protrude alongside the metal rings of the electrode array, therefore forming an electro-optical array of electrode-waveguide pairs arranged in an alternating fashion for best hybrid stimulation access to the auditory nerve. The proposed hybrid neurostimulation methodology and device prototype concept, based on the research findings presented herein, provide major research contribution for a next generation cochlear implants and sound modulation technology.

.

7. Future Work

7.1. *In-Vivo* Applications

Based on this research and recommendations, one can explore various *in-vivo* applications of interest where hybrid electro-plasmonic neurostimulation can be implemented. For example, just to mention few, Cochlear implants can be transformed using this hybrid technology, as previously elaborated in detail in the conclusions section of this work. Also, a new generation Myography stimulators can be designed to implement the hybrid electro-plasmonic methodology for stimulation and treatment of peripheral neuropathy; an alternative to current electromyography.

Rationale: Currently, electromyography (EMG) measures muscle response or electrical activity in response to a nerve's stimulation of the muscle. The test is used to help detect neuromuscular abnormalities. During the test, one or more small needles (electrodes) are inserted through the skin into the muscle to detect peripheral neuropathy, but this method cannot do specific point stimulation. The primary work in the aim can be focused on developing a hybrid stimulation-based method to detect/diagnose peripheral neuropathy, as it can be much more spatially focused. More specifically, work can center on stimulating a primary nerve of one's choice in rat animal models.

Future experimental design can be done to work with Sprague-Dawley rat animal models for in-vivo sciatic nerve stimulation experiments. An incision in the selected muscle would expose the main trunk of the nerve of interest. The nanoelectrode could be placed at the

stimulating site and a 532 nm green laser focused on the tip of the nanoelectrode using a 50 μm inner diameter optical fiber or fiber dots or waveguides as a light source. A standard neural cuff could be used to record compound nerve action potential and compound muscle action potential[82-84]. Electrical stimulation experiments shall be done before and after the optical and/or hybrid stimulation using a tungsten electrical electrode for stimulation and the standard cuff for recording. In the long run, one can examine the plasmonic and/or hybrid stimulation for chronic animal pain models to test the viability in pain management. These results will facilitate the development of new and improved implantable stimulators by reducing the required electrical and possibly laser power, and offer spatially precise and safer stimulation modality. This research will open doors for a new era of hybrid stimulation with smart i.e. artificial intelligence equipped wearable sensors and stimulation prosthetics or implantable neural modulation medical devices that can improve how we manage and treat neural response deficiencies and response specific and tunable for each patient.

Animal Protocols Disclaimer

All the animal protocols and procedures were approved by the University of South Florida Institutional Animal Care and Use Committee (IACUC) and are consistent with US Federal and NIH guidelines, with the necessary training provided. The mouse tissue was provided by the laboratory of Prof. Thomas Taylor-Clark, College of Medicine Molecular Pharmacology & Physiology, University of South Florida, Tampa, FL.

References

1. Wang, Y.; Guo, L., Nanomaterial-Enabled Neural Stimulation. *Front Neurosci* **2016,** *10*, 69.

2. Deisseroth, K., Optogenetics: 10 Years of Microbial Opsins in Neuroscience. *Nat Neurosci* **2015,** *18* (9), 1213-1225.

3. Colombo, E.; Feyen, P.; Antognazza, M. R.; Lanzani, G.; Benfenati, F., Nanoparticles: A Challenging Vehicle for Neural Stimulation. *Front Neurosci* **2016,** *10*, 105.

4. Carvalho-de-Souza, J. L.; Treger, J. S.; Dang, B.; Kent, S. B.; Pepperberg, D. R.; Bezanilla, F., Photosensitivity of Neurons Enabled by Cell-Targeted Gold Nanoparticles. *Neuron* **2015,** *86* (1), 207-17.

5. Marino, A.; Arai, S.; Hou, Y.; Sinibaldi, E.; Pellegrino, M.; Chang, Y. T.; Mazzolai, B.; Mattoli, V.; Suzuki, M.; Ciofani, G., Piezoelectric Nanoparticle-Assisted Wireless Neuronal Stimulation. *Acs Nano* **2015,** *9* (7), 7678-89.

6. Chen, R.; Romero, G.; Christiansen, M. G.; Mohr, A.; Anikeeva, P., Wireless Magnetothermal Deep Brain Stimulation. *Science* **2015,** *347* (6229), 1477-80.

7. Eom, K.; Kim, J.; Choi, J. M.; Kang, T.; Chang, J. W.; Byun, K. M.; Jun, S. B.; Kim, S. J., Enhanced Infrared Neural Stimulation Using Localized Surface Plasmon Resonance of Gold Nanorods. *Small* **2014,** *10* (19), 3853-3857.

8. Yong, J.; Needham, K.; Brown, W. G.; Nayagam, B. A.; McArthur, S. L.; Yu, A.; Stoddart, P. R., Gold-Nanorod-Assisted Near-Infrared Stimulation of Primary Auditory Neurons. *Adv Healthc Mater* **2014,** *3* (11), 1862-8.

9. Chen, S.; Weitemier, A. Z.; Zeng, X.; He, L.; Wang, X.; Tao, Y.; Huang, A. J. Y.; Hashimotodani, Y.; Kano, M.; Iwasaki, H.; Parajuli, L. K.; Okabe, S.; Teh, D. B. L.; All, A. H.; Tsutsui-Kimura, I.; Tanaka, K. F.; Liu, X.; McHugh, T. J., Near-Infrared Deep Brain Stimulation *via* Upconversion Nanoparticle-Mediated Optogenetics. *Science* **2018,** *359* (6376), 679-684.

10. Yoo, S.; Hong, S.; Choi, Y.; Park, J. H.; Nam, Y., Photothermal Inhibition of Neural Activity With Near-Infrared-Sensitive Nanotransducers. *Acs Nano* **2014,** *8* (8), 8040-9.

11. Li, W.; Luo, R.; Lin, X.; Jadhav, A. D.; Zhang, Z.; Yan, L.; Chan, C. Y.; Chen, X.; He, J.; Chen, C. H.; Shi, P., Remote Modulation of Neural Activities *via* Near-Infrared Triggered Release of Biomolecules. *Biomaterials* **2015,** *65*, 76-85.

12. Pappas, T. C.; Wickramanyake, W. M.; Jan, E.; Motamedi, M.; Brodwick, M.; Kotov, N. A., Nanoscale engineering of a cellular interface with semiconductor nanoparticle films for photoelectric stimulation of neurons. *Nano Lett* **2007,** *7* (2), 513-9.

13. Duke, A. R.; Cayce, J. M.; Malphrus, J. D.; Konrad, P.; Mahadevan-Jansen, A.; Jansen, E. D., Combined Optical and Electrical Stimulation of Neural Tissue *in vivo*. *Journal of Biomedical Optics* **2009,** *14* (6), 060501.

14. Zhao, Y.; Larimer, P.; Pressler, R. T.; Strowbridge, B. W.; Burda, C., Wireless Activation of Neurons in Brain Slices Using Nanostructured Semiconductor Photoelectrodes. *Angewandte Chemie International Edition* **2009,** *48* (13), 2407-2410.

15. Parameswaran, R.; Carvalho-de-Souza, J. L.; Jiang, Y.; Burke, M. J.; Zimmerman, J. F.; Koehler, K.; Phillips, A. W.; Yi, J.; Adams, E. J.; Bezanilla, F., Photoelectrochemical Modulation of Neuronal Activity With Free-standing Coaxial Silicon Nanowires. *Nature Nanotechnology* **2018,** *13* (3), 260.

16. Rettenmaier, A.; Lenarz, T.; Reuter, G., Nanosecond Laser Pulse Stimulation of Spiral Ganglion Neurons and Model Cells. *Biomedical Optics Express* **2014,** *5* (4), 1014-1025.

17. Zhang, J.; Atay, T.; Nurmikko, A. V., Optical Detection of Brain Cell Activity Using Plasmonic Gold Nanoparticles. *Nano Letters* **2009,** *9* (2), 519-524.

18. Shapiro, M. G.; Homma, K.; Villarreal, S.; Richter, C.-P.; Bezanilla, F., Infrared Light Excites Cells By Changing Their Electrical Capacitance. *Nature Communications* **2012,** *3*, 736.

19. Wells, J.; Kao, C.; Mariappan, K.; Albea, J.; Jansen, E. D.; Konrad, P.; Mahadevan-Jansen, A., Optical stimulation of neural tissue in vivo. *Optics letters* **2005,** *30* (5), 504-506.

20. Nakatsuji, H.; Numata, T.; Morone, N.; Kaneko, S.; Mori, Y.; Imahori, H.; Murakami, T., Thermosensitive Ion Channel Activation in Single Neuronal Cells by Using Surface-Engineered Plasmonic Nanoparticles. *Angewandte Chemie International Edition* **2015,** *54* (40), 11725-11729.

21. Eom, K.; Byun, K. M.; Jun, S. B.; Kim, S. J.; Lee, J., Theoretical Study on Gold-Nanorod-Enhanced Near-Infrared Neural Stimulation. *Biophysical journal* **2018,** *115* (8), 1481-1497.

22. Wilson, B. S.; Dorman, M. F., Cochlear implants: a remarkable past and a brilliant future. *Hearing research* **2008,** *242* (1-2), 3-21.

23. Wilson, B. S., Finley, C. C., Lawson, D. T., Wolford, R. D., Eddington, D. K., and Rabinowitz, W.M., Better speech recognition with cochlear implants. *Nature* **1991**, 352(6332):236–238.

24. Shire, D. B. e. a., Development and Implantation of a Minimally Invasive Wireless Subretinal Neurostimulator. *IEEE Transactions on Biomedical Engineering* **2009**, Volume: 56, Issue: 10, 2502 - 2511.

25. Hornig, R., Laube, T., Walter, P., Velikay-Parel, M., Bornfeld, N., Feucht, M., Akguel, H., Rssler, G., Alteheld, N., Notarp, D. L., Wyatt, J., and Richard, G., A method and technical equipment for an acute human trial to evaluate retinal implant technology. *Journal of Neural Engineering* **2005**, 2(1):S129.

26. Bosch, J. L. H. R. a. G. J., Sacral (S3) Segmental Nerve Stimulation as a Treatment for Urge Incontinence in Patients with Detrusor Instability: Results of Chronic Electrical Stimulation using an Implantable Neural Prosthesis. *The Journal of Urology* **1995**, Volume 154, Issue 2, Pages 504-507.

27. Long, D. M. e. a., Electrical Stimulation of the Spinal Cord and Peripheral Nerves for Pain Control. *Appl Neurophysiol* **1981**, 44:207–217.

28. Olusanya B. O., N. K. J., Saunders J. E., The global burden of disabling hearing impairment: a call to action. *Bull World Health Organ.* **2014**, 92(5): 367–373.

29. Saunders J, B. D., Cochlear implantation in developing countries as humanitarian service: physician attitudes and recommendations for best practice. . *Otolaryngol Head Neck Surg.* **2011**, 145:74–9.

30. Kral A., O. D. G. M., Profound deafness in childhood. *N Engl J Med.* **2010**, 363:1438–50.

31. Friesen LM, S. R., Baskent D, Wang X., Speech recognition in noise as a function of the number of spectral channels comparison of acoustic hearing and cochlear implants. *J Acoust Soc Am.* **2001**, 110:1150–1163.

32. O'Leary, S. J., Richardson, R. R., and McDermott, H. J., Principles of design and biological approaches for improving the selectivity of cochlear implant electrodes. *Journal of Neural Engineering* **2009**, 6(5):055002.

33. Limb, C. J. a. R., A. T., Technological, biological, and acoustical constraints to music perception in cochlear implant users. Music: A window into the hearing brain. *Hearing Research* **2014**, 308(0):13 – 26.

34. Firszt, J. B., Koch, D. B., Downing, M., and Litvak, L., Current steering creates addiadditional pitch percepts in adult cochlear implant recipients. *Otology & Neurotology* **2007**, 28(5):629-636.

35. Richter CP, M. A., Wells JD, Jansen ED, Walsh JT., Neural stimulation with optical radiation. . *Laser Photonics Rev.* **2011**, 5(1):68–80.

36. Fenno L, Y. O., Deisseroth K., The Development and Application of Optogenetics. *Annu Rev Neurosci.* **2011**, 34(1):389–412.

37. Richter, C.-P. e. a., Optical stimulation of auditory neurons: Effects of acute and. *Hear Res* **2008**, 242(1-2): 42–51.

38. Izzo, A. D., Richter, C.-P., Jansen, E. D., and Walsh, J. T., Laser stimulation of the auditory nerve. *Lasers in Surgery and Medicine* **2006**, 38(8):745–753.

39. Izzo, A. D., Suh, E., Walsh, J. T., Whitlon, D. S., Richter, C.-P., and Pathria, J., Selectivity of neural stimulation in the auditory system: a comparison of optic and electric stimuli. *Journal of biomedical optics* **2007**, 12(2):021008–021008.

40. Rajguru, S. M., Matic, A. I., Robinson, A. M., Fishman, A. J., Moreno, L. E., Bradley, A., Vujanovic, I., Breen, J., Wells, J. D., Bendett, M., et al., Optical cochlear implants: evaluation of surgical approach and laser parameters in cats. *Hearing research* **2010**, 269(1):102–111.

41. Littlefield, P. D., Vujanovic, I., Mundi, J., Matic, A. I., and Richter, C. P., Laser s timulation of single auditory nerve fibers. *The Laryngoscope* **2010**, 120(10):2071–2082.

42. Wells, J., Kao, C., Konrad, P., Milner, T., Kim, J., Mahadevan-Jansen, A., and Jansen, E. D., Biophysical mechanisms of transient optical stimulation of peripheral nerve. *Biophysical Journal* **2007**, Vol.93 2567–2580.

43. Wells, J., Kao, C., Jansen, E. D., Konrad, P., and Mahadevan-Jansen, A., Application of infrared light for in vivo neural stimulation. *Journal of Biomedical Optics* **2005**, 10(6):064003–064003–12.

44. Shapiro, H., Villarreal, Richter, Bezanilla, Infrared light excites cells by changing their electrical capacitance. *Nature Communications* **2012**, Article number: 736

45. Duke, A. R. e. a., Combined optical and electrical stimulation of neural tissue in vivo. *J. Biomed. Opt.* **2009**, 14, 060501.

46. Bazard, P.; Frisina, R. D.; Walton, J. P.; Bhethanabotla, V. R., Nanoparticle-based Plasmonic Transduction for Modulation of Electrically Excitable Cells. *Scientific Reports* **2017,** *7* (1), 7803.

47. Rea, P., *Essential Clinical Anatomy of the Nervous System*. Elsevier/AP, Academic Press is an imprint of Elsevier: Amsterdam ; Boston, 2015.

48. Waldman, S. D., *Pain Management E-Book*. 2 ed.; Elsevier Health Sciences: 2011; p 1145-1151.

49. Kovalevich, J. a. L., D., Considerations for the Use of SH-SY5Y Neuroblastoma Cells in Neurobiology. In *Neuronal Cell Culture: Methods and Protocols*, Springer IP AG.: 2013; pp volume 1078, 9-21

.

50. Phlman, S., Ruusala, A.-I., Abrahamsson, L., Mattsson, M. E., and Esscher, T., Retinoic acid-induced differentiation of cultured human neuroblastoma cells: a comparison with phorbolester-induced differentiation. *Cell Differentiation* **1984**, 14(2):135 – 144.

51. Bazard, P., Frisina, R. D., Walton, J. P., Bhethanabotla, V. R., Plasmonic Stimulation of Electrically Excitable Cells. *Scientific_Reports* **2017**, DOI:10.1038/s41598-017-08141-4.

52. Nath, N.; Chilkoti, A., A Colorimetric Gold Nanoparticle Sensor To Interrogate Biomolecular Interactions in Real Time on a Surface. *Analytical Chemistry* **2002**, 74(3):504–509.

53. Alshammari, A.; Köckritz, A.; Kalevaru, V. N.; Bagabas, A.; Martin, A., Influence of Single Use and Combination of Reductants on the Size, Morphology and Growth Steps of Gold Nanoparticles in Colloidal Mixture. *Open J. Phys. Chem* **2012,** *2* (4), 252-261.

54. Alshammari, A., Köckritz, A., Kalevaru, V. N., Bagabas, A., Martin, A., Influence of Single Use and Combination of Reductants on the Size, Morphology and Growth Steps of Gold Nanoparticles in Colloidal Mixture. *Open Journal of Physical Chemistry* **2012**, 2, 252-261

55. Tyagi, H.; Kushwaha, A.; Kumar, A.; Aslam, M., A facile pH controlled citrate-based reduction method for gold nanoparticle synthesis at room temperature. *Nanoscale research letters* **2016,** *11* (1), 362.

56. Kimling, J.; Maier, M.; Okenve, B.; Kotaidis, V.; Ballot, H.; Plech, A., Turkevich method for gold nanoparticle synthesis revisited. *The Journal of Physical Chemistry B* **2006,** *110* (32), 15700-15707.

57. Turkevich, J.; Stevenson, P. C.; Hillier, J., A study of the nucleation and growth processes in the synthesis of colloidal gold. *Discussions of the Faraday Society* **1951,** *11*, 55-75.

58. Shukla, R.; Bansal, V.; Chaudhary, M.; Basu, A.; Bhonde, R. R.; Sastry, M., Biocompatibility of gold nanoparticles and their endocytotic fate inside the cellular compartment: a microscopic overview. *Langmuir* **2005,** *21* (23), 10644-10654.

59. Nath, N.; Chilkoti, A., A Colorimetric Gold Nanoparticle Sensor to Interrogate Biomolecular Interactions in Real Time on a Surface. *Analytical Chemistry* **2002,** *74* (3), 504-509.

60. Oesterle, A., Pipette Cookbook 2018: P-97 & P-1000 Micropipette Pullers. In *California: Sutter Instrument* [Online] 2015; pp. 108, 5-33. http://www.sutter.com/contact/faqs/pipette_cookbook.pdf.

61. Instrument, S., Patch Pipettes.

62. Lewinski, N.; Colvin, V.; Drezek, R., Cytotoxicity of nanoparticles. *small* **2008,** *4* (1), 26-49.

63. Coronado, E. A.; Encina, E. R.; Stefani, F. D., Optical properties of metallic nanoparticles: manipulating light, heat and forces at the nanoscale. *Nanoscale* **2011,** *3* (10), 4042-4059.

64. Huang, X.; El-Sayed, M. A., Gold nanoparticles: Optical properties and implementations in cancer diagnosis and photothermal therapy. *Journal of advanced research* **2010,** *1* (1), 13-28.

65. Horikoshi S., S. N., Microwaves in Nanoparticle Synthesis: Fundamentals and Applications. In *Microwaves in Nanoparticle Synthesis: Fundamentals and Applications*. Horikoshi S., S. N., Ed. John Wiley & Sons: 2013; pp 352 (1-24).

66. Migliori, B.; Di Ventra, M.; Kristan Jr, W., Photoactivation of neurons by laser-generated local heating. *AIP advances* **2012,** *2* (3), 032154.

67. Martino, N.; Feyen, P.; Porro, M.; Bossio, C.; Zucchetti, E.; Ghezzi, D.; Benfenati, F.; Lanzani, G.; Antognazza, M. R., Photothermal cellular stimulation in functional bio-polymer interfaces. *Scientific reports* **2015,** *5*, 8911.

68. Plaksin, M.; Shapira, E.; Kimmel, E.; Shoham, S., Thermal transients excite neurons through universal intramembrane mechanoelectrical effects. *Physical Review X* **2018,** *8* (1), 011043.

69. Bec, J. M.; Albert, E. S.; Marc, I.; Desmadryl, G.; Travo, C.; Muller, A.; Chabbert, C.; Bardin, F.; Dumas, M., Characteristics of laser stimulation by near infrared pulses of retinal and vestibular primary neurons. *Lasers in surgery and medicine* **2012,** *44* (9), 736-745.

70. Cayce, J. M.; Friedman, R. M.; Chen, G.; Jansen, E. D.; Mahadevan-Jansen, A.; Roe, A. W., Infrared neural stimulation of primary visual cortex in non-human primates. *Neuroimage* **2014,** *84*, 181-190.

71. Cayce, J. M.; Friedman, R. M.; Jansen, E. D.; Mahavaden-Jansen, A.; Roe, A. W., Pulsed infrared light alters neural activity in rat somatosensory cortex in vivo. *Neuroimage* **2011,** *57* (1), 155-166.

72. Wells, J.; Kao, C.; Konrad, P.; Milner, T.; Kim, J.; Mahadevan-Jansen, A.; Jansen, E. D., Biophysical mechanisms of transient optical stimulation of peripheral nerve. *Biophysical journal* **2007,** *93* (7), 2567-2580.

73. Izzo, A. D.; Richter, C. P.; Jansen, E. D.; Walsh Jr, J. T., Laser stimulation of the auditory nerve. *Lasers in Surgery and Medicine: The Official Journal of the American Society for Laser Medicine and Surgery* **2006,** *38* (8), 745-753.

74. Littlefield, P. D.; Vujanovic, I.; Mundi, J.; Matic, A. I.; Richter, C. P., Laser stimulation of single auditory nerve fibers. *The Laryngoscope* **2010,** *120* (10), 2071-2082.

75. Teudt, I. U.; Nevel, A. E.; Izzo, A. D.; Walsh Jr, J. T.; Richter, C. P., Optical stimulation of the facial nerve: a new monitoring technique? *The Laryngoscope* **2007,** *117* (9), 1641-1647.

76. Izzo, A. D.; Walsh Jr, J. T.; Ralph, H.; Webb, J.; Bendett, M.; Wells, J.; Richter, C.-P., Laser stimulation of auditory neurons: effect of shorter pulse duration and penetration depth. *Biophysical journal* **2008,** *94* (8), 3159-3166.

77. Richter, C.-P.; Rajguru, S. M.; Matic, A. I.; Moreno, E. L.; Fishman, A. J.; Robinson, A. M.; Suh, E.; Walsh Jr, J. T., Spread of cochlear excitation during stimulation with pulsed infrared radiation: inferior colliculus measurements. *Journal of neural engineering* **2011,** *8* (5), 056006.

78. Rajguru, S. M.; Richter, C. P.; Matic, A. I.; Holstein, G. R.; Highstein, S. M.; Dittami, G. M.; Rabbitt, R. D., Infrared photostimulation of the crista ampullaris. *The Journal of physiology* **2011,** *589* (6), 1283-1294.

79. Farah, N.; Brosh, I.; Butson, C. R.; Shoham, S., Photo-thermal neural excitation by extrinsic and intrinsic absorbers: a temperature-rate model. *arXiv preprint arXiv:1201.4617* **2012**.

80. Dorman, M. F.; Gifford, R. H.; Spahr, A. J.; McKarns, S. A., The benefits of combining acoustic and electric stimulation for the recognition of speech, voice and melodies. *Audiology and Neurotology* **2008,** *13* (2), 105-112.

81. Wolfe, J.; Morais, M.; Schafer, E., Speech recognition of bimodal cochlear implant recipients using a wireless audio streaming accessory for the telephone. *Otology & Neurotology* **2016,** *37* (2), e20-e25.

82. Rodri, F. J. e. a., Polyimide cuff electrodes for peripheral nerve stimulation. *Journal of neuroscience methods* **2000**, 98, 105-118.

83. Mosconi, T. K., L., Fixed-diameter polyethylene cuffs applied to the rat sciatic nerve induce a painful neuropathy: ultrastructural morphometric analysis of axonal alterations. *Pain* **1996**, 64, 37-57.

84. Fugleholm, K., Schmalbruch, H. & Krarup, C., Early peripheral nerve regeneration after crushing, sectioning, and freeze studied by implanted electrodes in the cat. *The Journal of neuroscience* **1994**, 14, 2659-2673.